

# Detection and replication of epistasis influencing transcription in humans

Gibran Hemani<sup>1,2,\*</sup>, Konstantin Shakhbazov<sup>1,2</sup>, Harm-Jan Westra<sup>3</sup>,  
Tonu Esko<sup>4,5,6</sup>, Anjali K Henders<sup>7</sup>, Allan F McRae<sup>1,2</sup>, Jian Yang<sup>1</sup>,  
Greg Gibson<sup>8</sup>, Nicholas G Martin<sup>7</sup>, Andres Metspalu<sup>4</sup>, Lude  
Franke<sup>3</sup>, Grant W Montgomery<sup>7,+</sup>, Peter M Visscher<sup>1,2,+</sup>, and  
Joseph E Powell<sup>1,2,+</sup>

<sup>1</sup>Queensland Brain Institute, University of Queensland, Brisbane, QLD, Australia. <sup>2</sup>University of Queensland Diamantina Institute, University of Queensland, Princess Alexandra Hospital, Brisbane, Queensland, Australia. <sup>3</sup>Department of Genetics, University Medical Center Groningen, University of Groningen, Hanzeplein 1, Groningen, the Netherlands. <sup>4</sup>Estonian Genome Center, University of Tartu, Tartu, 51010, Estonia. <sup>5</sup>Medical and Population Genetics, Broad Institute, Cambridge, MA, 02142, US. <sup>6</sup>Divisions of Endocrinology, Children's Hospital, Boston, MA, 02115, US. <sup>7</sup>Queensland Institute of Medical Research, Brisbane, Queensland, Australia. <sup>8</sup>School of Biology and Centre for Integrative Genomics, Georgia Institute of Technology, Atlanta, Georgia United States of America. <sup>+</sup>These authors contributed equally. <sup>\*</sup>Corresponding author: g.hemani@uq.edu.au

## Abstract

Epistasis is the phenomenon whereby one polymorphism’s effect on a trait depends on other polymorphisms present in the genome. The extent to which epistasis influences complex traits<sup>1</sup> and contributes to their variation<sup>2,3</sup> is a fundamental question in evolution and human genetics. Though often demonstrated in artificial gene manipulation studies in model organisms,<sup>4,5</sup> and some examples have been reported in other species,<sup>6</sup> few examples exist for epistasis amongst natural polymorphisms in human traits.<sup>7,8</sup> Its absence from empirical findings may simply be due to low incidence in the genetic control of complex traits,<sup>2,3</sup> but an alternative view is that it has previously been too technically challenging to detect due to statistical and computational issues.<sup>9</sup> Here we show that, using advanced computation<sup>10</sup> and a gene expression study design, many instances of epistasis are found between common single nucleotide polymorphisms (SNPs). In a cohort of 846 individuals with 7339 gene expression levels measured in peripheral blood, we found 501 significant pairwise interactions between common SNPs influencing the expression of 238 genes ( $p < 2.91 \times 10^{-16}$ ). Replication of these interactions in two independent data sets<sup>11,12</sup> showed both concordance of direction of epistatic effects ( $p = 5.56 \times 10^{-31}$ ) and enrichment of interaction  $p$ -values, with 30 being significant at a conservative threshold of  $p < 0.05/501$ . Forty-four of the genetic interactions are located within 2Mb of regions of known physical chromosome interactions<sup>13</sup> ( $p = 1.8 \times 10^{-10}$ ). Epistatic networks of three SNPs or more influence the expression levels of 129 genes, whereby one *cis*-acting SNP is modulated by several *trans*-acting SNPs. For example MBNL1 is influenced by an additive effect at rs13069559 which itself is masked by *trans*-SNPs on 14 different chromosomes, with nearly identical genotype-phenotype (GP) maps for each *cis-trans* interaction. This study presents the first evidence for multiple instances of segregating common polymorphisms interacting to influence human traits.

## Main text

In the genetic analysis of complex traits it is usual for SNP effects to be estimated using an additive model where they are assumed to contribute independently and cumulatively to the mean of a trait. This framework has been successful in identifying thousands of associations.<sup>14</sup> But to date, though its contribution to phenotypic variance is frequently the subject of debate,<sup>1-3</sup> there is little empirical exploration of the role that epistasis plays in the architecture of complex traits in humans.<sup>7,8</sup> Beyond the prism of human association studies there is evidence for epistasis, not only at the molecular scale from artificially induced mutations<sup>4</sup> but also at the evolutionary scale in fitness adaptation<sup>15</sup> and speciation.<sup>16</sup>

Methods are now available to overcome the computational problems involved in searching for epistasis, but its detection still remains problematic due to reduced statistical power. For example, increased dependence on linkage disequilibrium (LD) between causal SNPs and observed SNPs,<sup>17,18</sup> increased model

complexity in fitting interaction terms,<sup>19</sup> and more extreme significance thresholds to account for increased multiple testing<sup>9</sup> all make it more difficult to detect epistasis in comparison to additive effects. Thus, with small genetic effect sizes, as is expected in most complex traits of interest,<sup>14</sup> the power to detect epistasis diminishes rapidly. There are two simple ways to overcome this problem. One is by using extremely large sample sizes;<sup>20</sup> another is by analysing traits that are likely to have large effect sizes among common variants. Because our focus was to ascertain the extent to which instances of epistasis arises from natural genetic variation we designed a study around the latter approach and searched for epistatic genetic effects that influence gene expression levels. Transcription levels can be measured for thousands of genes and like most complex diseases, these expression traits are typically heritable.<sup>21</sup> But unlike complex diseases, genetic associations with gene expression commonly have very large effect sizes that explain large proportions of the genetic variance,<sup>22</sup> making them good candidates to search for epistasis, should it exist.

In our discovery dataset (Brisbane Systems Genetics Study, BSGS<sup>23</sup>) of 846 individuals genotyped at 528,509 SNPs, we used a two stage approach to identify genetic interactions. First, we exhaustively test every pair of SNPs for pairwise effects against each of 7339 expression traits in peripheral blood ( $1.03 \times 10^{15}$  statistical tests, family-wise error rate of 5% corresponding to a significance threshold of  $p < 2.91 \times 10^{-16}$ , Methods). Second, we filtered the SNP pairs from stage 1 on LD and genotype class counts, and tested the remaining pairwise effects for significant interaction terms and used a Bonferroni correction for multiple testing (estimated type 1 error rate  $0.05 \leq \alpha \leq 0.14$ , Methods, Supplementary Figure S1). Using this design we identified 501 putative genetic interactions influencing the expression levels of 238 genes (Supplementary Table S1). We used strict quality control measures to avoid statistical associations being driven by technical artifacts (Methods). However it remains possible that unexplained technical artifacts may have led to the significant discovery interactions. Of the 501 discovery interactions, 434 had available data and passed filtering (Methods) in two independent replication datasets, Fehrmann<sup>12</sup> and the Estonian Genomics Centre University of Tartu (EGCUT),<sup>11</sup> in which we saw convincing evidence for replication. We used the summary statistics from the replication datasets to perform a meta analysis to obtain an independent  $p$ -value for the putative interactions, and 30 were significant after applying a Bonferroni correction for multiple testing (5% significance threshold  $p < 0.05/501$ , Table 1). To quantify the similarity of GP maps between the independent datasets (Figure 1) we decomposed the genetic effects of each of the SNP pairs into orthogonal additive, dominance and epistatic effects ( $A1$ ,  $A2$ ,  $D1$ ,  $D2$ ,  $A1 \times A2$ ,  $A1 \times D2$ ,  $D1 \times A2$ ,  $D1 \times D2$ ) and tested for concordance of the sign of the most significant effect (Supplementary Table S3, Methods). Sign concordance between the discovery and both replication datasets was observed in 22 out of the 30 significantly replicated interactions (expected value = 7.5 under the null hypothesis of no interactions,  $p = 3.76 \times 10^{-8}$ ).

In addition, using the meta analysis from the replication samples only, we observed that 316 of the remaining 404 discovery SNP pairs had replication

interaction  $p$ -values more extreme than the 2.5% confidence interval of the quantile-quantile plot against the null hypothesis of no interactions where  $p$ -values are assumed to be uniformly distributed ( $p \ll 1.0 \times 10^{-16}$ , Figure 2 and Supplementary Figure S2). Concordance of the direction of the effect of the largest variance component was also highly significant ( $p = 5.71 \times 10^{-31}$ , Supplementary Table S3). The congruence of the epistatic networks in discovery and replication datasets is shown in Figure 3, demonstrating that these complex genetic patterns are common even across independent datasets. A further replication was attempted using the Centre for Health Discovery and Wellbeing (CHDWB) dataset,<sup>24</sup> but only 20 of the SNP pairs passed filtering because the sample size was small ( $n = 139$ ), and likely due to insufficient power we found no evidence for replication (Supplementary Figure S6). It should be noted that although it is a necessary step to establish the veracity of the interactions from the discovery set, replication of epistatic effects in independent samples is difficult in practice due to LD (Methods).

Though seldom the focus of association studies, SNPs with known main effects are often tested for  $A \times A$  genetic interactions,<sup>9</sup> but our analysis suggests this is unlikely to be the best strategy for its detection. The majority of our discovery interactions comprised of one SNP that was significantly associated with the gene expression level in the discovery dataset, and one SNP that had no previous association<sup>22</sup> (439 out of 501, Methods). Only nine interactions were between SNPs that both had known main effects while 64 were between SNPs that had no known main effects. Additionally, we observed that the largest epistatic variance component for the 501 interactions was equally divided amongst  $A \times A$ ,  $A \times D$ ,  $D \times A$  and  $D \times D$  at the discovery stage ( $p = 0.22$  for departure from expectation). This is not surprising because these patterns of epistasis used for statistical decomposition are simply convenient orthogonal parameterisations of a two locus model, and are not intended to model biological function.<sup>25</sup>

Of the discovery interactions, 26 were *cis-cis* acting (within 1Mb of the transcription start site, mean distance between SNPs was 0.53Mb), 462 were *cis-trans*-acting, and 13 were *trans-trans*-acting. We observed a wide range of significant GP maps (Figure 1) but the most common pattern of epistasis that we detected involved a *trans*-SNP masking the effect of an additive *cis*-SNP. For example, MBNL1 (involved in RNA modification and regulation of splicing<sup>26</sup>) has a *cis* effect at rs13069559 which in turn is controlled by 13 *trans*-SNPs and one *cis*-SNP that each exhibit a masking pattern, such that when the *trans*-SNP is homozygous for the masking allele the decreasing allele of the *cis*-SNP no longer has an effect (Supplementary Figure S10). Each of these interactions has evidence for replication in at least one dataset and six are significantly replicated at the Bonferroni level (Supplementary Figure S3). We see similar epistatic networks involving multiple (eight or more) *trans*-acting SNPs for other gene expression levels too, for example TMEM149 (Supplementary Figure S11), NAPRT1 (Supplementary Figure S12), TRAPPC5 (Supplementary Figure S13), and CAST (Supplementary Figure S14). We observed that from pedigree analysis these five gene expression phenotypes had non-additive variance component

estimates within the 95th percentile of the 17,994 gene expression phenotypes that were analysed previously<sup>22</sup> (Supplementary Table S2, Methods).

In total the 501 interactions comprised 781 unique SNPs, which we analysed for functional enrichment (Methods). We tested the SNPs for cell-type specific overlap with transcriptionally active chromatin regions, tagged by histone-3-lysine-4,tri-methylation (H3K4me3) chromatin marks, in 34 cell types<sup>27</sup> (Supplementary Figure S5). There was significant enrichment for *cis*-acting SNPs in haematopoietic cell types only ( $p < 1 \times 10^{-4}$  for the three tissues with the strongest enrichment after adjusting for multiple testing). However *trans*-acting SNPs did not show any tissue specific enrichment ( $p > 0.1$  for all tissues). This difference between *cis* and *trans* SNPs suggests different roles in epistatic interactions where tissue specificity is provided by the *cis* SNPs. There is also enrichment for *cis*-SNPs to be localised in regions with regulatory genomic features as measured by chromatin states<sup>28</sup> (Supplementary Figure S4).

We also demonstrate physical organisation of interacting loci within the cell, suggesting a mechanism by which biological function can lead to epistatic genetic variance. It has been shown that different chromosomal regions spatially colocalise in the cell through chromatin interactions.<sup>13</sup> We cross-referenced our epistatic SNPs with a map of chromosome interacting regions ( $n = 96,139$ ) in K562 blood cell lines<sup>29</sup> (Methods) and found that 44 epistatic interactions mapped to within 5Mb ( $p < 1.8 \times 10^{-10}$ ), (Supplementary Figure S15). Interaction of distant loci may occur through physical proximity in transcriptional factories that organise across different chromosome regions and can regulate transcription of related genes.<sup>30</sup>

Quantifying the importance of epistasis in complex traits in humans remains an open question. Here we are able to identify 238 gene expression traits with at least one significant interaction given our experiment-wide threshold, where the minimum estimated variance explained by the epistatic effects of any interaction was 2.1% of phenotypic variance. Taking results from our previously published eQTL<sup>23</sup> we calculated that 1848 of the 7339 gene expression levels analysed were influenced by additive effects where the estimated additive variance of a locus was 2.1% or greater. Thus, we can infer that the number of instances of large additive effects is significantly greater than the number of instances of large epistatic effects.

In terms of their contribution to complex traits a more important metric might be the proportion of the variance that the epistatic loci explain.<sup>2</sup> Taking all additive effects detected in Powell *et al* (2012) that have additive variance explaining 2.1% or greater of phenotypic variance, we calculated that the proportion of total phenotypic variance of all 7339 gene expression levels explained by additive effects alone was 2.16%. By contrast, the estimated epistatic variance from the interacting SNPs detected in this study on average explain a total of 0.22% of phenotypic variance, approximately ten times lower than the estimated additive variance. There are several caveats to this comparison which we discuss in the Methods.

Overall, we have demonstrated that it is possible to identify and replicate epistasis in complex traits amongst common human variants, despite the rela-

tive contribution of pairwise epistasis to phenotypic variation being small. The bioinformatic analysis of the significant epistatic loci suggests that there are a large number of possible mechanisms that can lead to non-additive genetic variation. Further research into such epistatic effects may provide a useful framework for understanding molecular mechanisms and complex trait variation in greater detail. With computational techniques and data now widely available the search for epistasis in larger datasets for traits of broader interest is warranted.

## Methods Summary

We searched for pairwise epistasis exhaustively in the BSGS discovery dataset,<sup>23</sup> which comprises 846 individuals who are genotyped at 528,509 autosomal SNPs. Each individual had gene expression levels measured in peripheral blood at 7,339 probes representing 6,158 RefSeq genes (significant expression in  $\geq 90\%$  of individuals). SNP pairs were modelled for full genetic effects, including marginal additive and dominance at both SNPs plus four interaction terms. We used permutation analysis to calculate an experiment-wide significance threshold of  $T_e = 2.91 \times 10^{-16}$  at the 5% family-wise error rate (FWER). All SNP pairs with LD  $r^2 > 0.1$  and  $D'^2 > 0.1$  were removed to minimise the possibility of haplotype effects. All SNP pairs were required to have at least five data points in all nine genotype classes. If multiple SNP pairs were present on the same chromosomes for a particular expression trait then only the sentinel SNP pair was retained. Finally, a nested test contrasting the full genetic model against the marginal additive and dominance model was performed for each remaining SNP pair. The 501 significant SNP pairs were carried forward for replication in two independent datasets that used the same expression assays for analysing transcription in peripheral blood Fehrmann,<sup>12</sup>  $n = 1240$ ; EGCUT,<sup>11</sup> ( $n = 891$ ). A meta analysis on the interaction  $p$ -values from each replication dataset was performed to provide an overall replication statistic for each putative interaction.

## Acknowledgements

We are grateful to the volunteers for their generous participation in these studies. We thank Bill Hill, Chris Haley and Lars Ronnegard for helpful discussions and comments.

This work could not have been completed without access to high performance GPGPU compute clusters. We acknowledge iVEC for the use of advanced computing resources located at iVEC@UWA ([www.ivec.org](http://www.ivec.org)), and the Multimodal Australian ScienceS Imaging and Visualisation Environment (MASSIVE) ([www.massive.org.au](http://www.massive.org.au)). We also thank Jake Carroll and Irek Porebski from the Queensland Brain Institute Information Technology Group for HPC support.

The University of Queensland group is supported by the Australian National Health and Medical Research Council (NHMRC) grants 389892, 496667, 613601, 1010374 and 1046880, the Australian Research Council (ARC) grant

(DE130100691), and by National Institutes of Health (NIH) grants GM057091 and GM099568.

The QIMR researchers acknowledge funding from the Australian National Health and Medical Research Council (grants 241944, 389875, 389891, 389892, 389938, 442915, 442981, 496739, 496688 and 552485), the and the National Institutes of Health (grants AA07535, AA10248, AA014041, AA13320, AA13321, AA13326 and DA12854). We thank Anthony Caracella and Lisa Bowdler for technical assistance with the micro-array hybridisations.

The CHDWB study funding support from the Georgia Institute of Technology Research Foundation. The funders had no role in study design, data collection and analysis, decision to publish, or preparation of the manuscript

The Fehrmann study was supported by grants from the Celiac Disease Consortium (an innovative cluster approved by the Netherlands Genomics Initiative and partly funded by the Dutch Government (grant BSIK03009), the Netherlands Organization for Scientific Research (NWO-VICI grant 918.66.620, NWO-VENI grant 916.10.135 to L.F.), the Dutch Digestive Disease Foundation (MLDS WO11-30), and a Horizon Breakthrough grant from the Netherlands Genomics Initiative (grant 92519031 to L.F.). This project was supported by the Prinses Beatrix Fonds, VSB fonds, H. Kersten and M. Kersten (Kersten Foundation), The Netherlands ALS Foundation, and J.R. van Dijk and the Adessium Foundation. The research leading to these results has received funding from the European Communitys Health Seventh Framework Programme (FP7/2007-2013) under grant agreement 259867.

The EGCUT study received targeted financing from Estonian Government SF0180142s08, Center of Excellence in Genomics (EXCEGEN) and University of Tartu (SP1GVARENG). We acknowledge EGCUT technical personnel, especially Mr V. Soo and S. Smit. Data analyzes were carried out in part in the High Performance Computing Center of University of Tartu.

## **Author contributions**

G.H., J.E.P., P.M.V., and G.W.M. conceived and designed the study. G.H., J.E.P., K.S., H-J.W., and J.Y. performed the analysis. T.E. and A.M. provided the EGCUT data. A.K.H., A.F.M., G.W.M., N.G.M., and J.E.P. provided the BSGS data. H-J.W. and L.F. provided the Fehrmann data. G.H. and J.E.P. wrote the manuscript with the participation of all authors.

## **Author information**

The authors declare no financial competing interests.

## Tables

Table 1: Epistatic interactions significant at the Bonferroni level in two replication sets

	Gene (chr.)	SNP 1 (chr.)	SNP 2 (chr.)	BSGS <sup>2</sup>	Fehrmann <sup>3</sup>	EGCUT <sup>3</sup>	Meta <sup>4</sup>
1	ADK (10)	rs2395095 (10)	rs10824092 (10)	6.69 <sup>1</sup>	18.33 <sup>1</sup>	21.21 <sup>1</sup>	39.82 <sup>1</sup>
2	ATP13A1 (19)	rs4284750 (19)	rs873870 (19)	5.30	12.18	3.25	14.23
3	C21ORF57 (21)	rs9978658 (21)	rs11701361 (21)	9.42	6.08	16.36	21.67
4	CSTB (21)	rs9979356 (21)	rs3761385 (21)	11.99	25.20	16.72	42.27
5	CTSC (11)	rs7930237 (11)	rs556895 (11)	7.16	18.76	15.06	33.53
6	FN3KRP (17)	rs898095 (17)	rs9892064 (17)	16.16	28.24	29.39	59.95
7	GAA (17)	rs11150847 (17)	rs12602462 (17)	13.91	19.98	12.99	32.60
8	HNRPH1 (5)	rs6894268 (5)	rs4700810 (5)	15.38	8.55	3.01	10.37
9	LAX1 (1)	rs1891432 (1)	rs10900520 (1)	19.16	18.60	11.22	29.24
10	MBNL1 (3)	rs16864367 (3)	rs13079208 (3)	13.49	16.25	24.74	41.56
11	MBNL1 (3)	rs7710738 (5)	rs13069559 (3)	7.92	2.55	7.89	9.28
12	MBNL1 (3)	rs2030926 (6)	rs13069559 (3)	7.10	0.91	5.80	5.53
13	MBNL1 (3)	rs2614467 (14)	rs13069559 (3)	5.74	4.13	2.22	5.30
14	MBNL1 (3)	rs218671 (17)	rs13069559 (3)	7.63	0.62	5.82	5.23
15	MBNL1 (3)	rs11981513 (7)	rs13069559 (3)	7.71	0.43	5.36	4.58
16	MBP (18)	rs8092433 (18)	rs4890876 (18)	5.40	7.06	21.91	28.73
17	NAPRT1 (8)	rs2123758 (8)	rs3889129 (8)	8.45	15.12	16.08	30.77
18	NCL (2)	rs7563453 (2)	rs4973397 (2)	7.31	7.51	6.33	12.70
19	PRMT2 (21)	rs2839372 (21)	rs11701058 (21)	4.81	0.69	4.47	4.06
20	RPL13 (16)	rs352935 (16)	rs2965817 (16)	4.98	3.79	14.41	17.24
21	SNORD14A (11)	rs2634462 (11)	rs6486334 (11)	7.31	13.11	10.96	23.22
22	TMEM149 (19)	rs807491 (19)	rs7254601 (19)	12.16	81.55	45.78	145.78
23	TMEM149 (19)	rs8106959 (19)	rs6926382 (6)	5.80	3.06	8.80	10.72
24	TMEM149 (19)	rs8106959 (19)	rs914940 (1)	6.22	3.36	6.96	9.20
25	TMEM149 (19)	rs8106959 (19)	rs2351458 (4)	7.30	0.04	9.61	8.00
26	TMEM149 (19)	rs8106959 (19)	rs6718480 (2)	8.55	3.31	5.15	7.36
27	TMEM149 (19)	rs8106959 (19)	rs1843357 (8)	6.21	3.72	3.33	6.00
28	TMEM149 (19)	rs8106959 (19)	rs9509428 (13)	9.44	0.10	5.75	4.47
29	TRA2A (7)	rs7776572 (7)	rs11770192 (7)	8.23	3.19	1.89	4.09
30	VASP (19)	rs1264226 (19)	rs2276470 (19)	5.09	0.94	5.14	4.95

<sup>1</sup>  $-\log_{10} p$ -values for 4 *d.f.* interaction tests

<sup>2</sup> Discovery dataset

<sup>3</sup> Independent replication dataset

<sup>4</sup> Meta analysis of interaction terms between replication datasets only



## Figures

Figure 1: **Replication of GP maps in two independent populations**

The GP maps for each epistatic interaction that is significant at the Bonferroni level in both replication datasets are shown. Each GP map consists of nine tiles where each tile represents the expression level for that two-locus genotype class. Phenotypes are for gene transcript levels (dark coloured tiles = high expression, light coloured tiles = low expression). Columns of GP maps are for each independent dataset. Rows of GP maps are for each of 30 significantly replicated interactions at the Bonferroni level, corresponding to the rows in Table 1. There is a clear trend of the GP maps replicating across all three datasets.

Figure 2: **Q-Q plots of interaction  $p$ -values from replication datasets**

The top panel shows all 434 discovery SNPs that were tested for interactions. Observed  $p$ -values ( $y$ -axis,  $-\log_{10}$  scale) are plotted against the expected  $p$ -values ( $x$ -axis,  $-\log_{10}$  scale). The multiple testing correction threshold for significance following Bonferroni correction is denoted by a dotted line. The bottom panel shows the same data as the top panel but excluding the 30 interactions that were significant at the Bonferroni level in the replication datasets. The shaded grey area represents the 5% confidence interval for the expected distribution of  $p$ -values. Dark blue points represent  $p$ -values that exceed the confidence interval, light blue are within the confidence interval.

Figure 3: **Discovery and replication of epistatic networks**

All 434 putative genetic interactions (edges) with data common to discovery and replication sets is shown, where black nodes represent SNPs and red nodes represent traits (gene expression probes). Three hundred and forty-five interactions had  $p$ -values exceeding the 2.5% confidence interval following meta analysis of the replication data. The remaining 89 interactions that did not replicate are depicted in grey. It is evident that a large proportion of the complex networks identified in the discovery set also exist in independent populations. An interactive version of this graph can be found here: [http://kn3in.github.io/detecting\\_epi/](http://kn3in.github.io/detecting_epi/)

## References

- <sup>1</sup> Carlborg, O. & Haley, C. S. Epistasis: too often neglected in complex trait studies? *Nature Reviews Genetics* **5**, 618–25 (2004).
- <sup>2</sup> Hill, W. G., Goddard, M. E. & Visscher, P. M. Data and Theory Point to Mainly Additive Genetic Variance for Complex Traits. *PLoS Genetics* **4** (2008).
- <sup>3</sup> Crow, J. F. On epistasis: why it is unimportant in polygenic directional selection. *Philosophical transactions of the Royal Society of London. Series B, Biological sciences* **365**, 1241–4 (2010).
- <sup>4</sup> Costanzo, M. *et al.* The genetic landscape of a cell. *Science (New York, N.Y.)* **327**, 425–31 (2010).
- <sup>5</sup> Bloom, J. S., Ehrenreich, I. M., Loo, W. T., Lite, T.-L. V. o. & Kruglyak, L. Finding the sources of missing heritability in a yeast cross. *Nature* 1–6 (2013).
- <sup>6</sup> Carlborg, O., Jacobsson, L., Ahgren, P., Siegel, P. & Andersson, L. Epistasis and the release of genetic variation during long-term selection. *Nature Genetics* **38**, 418–420 (2006).
- <sup>7</sup> Strange, A. *et al.* A genome-wide association study identifies new psoriasis susceptibility loci and an interaction between HLA-C and ERAP1. *Nature Genetics* **42**, 985–90 (2010).
- <sup>8</sup> Evans, D. M. *et al.* Interaction between ERAP1 and HLA-B27 in ankylosing spondylitis implicates peptide handling in the mechanism for HLA-B27 in disease susceptibility. *Nature Genetics* **43** (2011).
- <sup>9</sup> Cordell, H. J. Detecting gene-gene interactions that underlie human diseases. *Nature Reviews Genetics* **10**, 392–404 (2009).
- <sup>10</sup> Hemani, G., Theocharidis, A., Wei, W. & Haley, C. EpiGPU: exhaustive pairwise epistasis scans parallelized on consumer level graphics cards. *Bioinformatics (Oxford, England)* **27**, 1462–5 (2011).
- <sup>11</sup> Metspalu, A. The Estonian Genome Project. *Drug Development Research* **62**, 97–101 (2004).
- <sup>12</sup> Fehrmann, R. S. N. *et al.* Trans-eQTLs reveal that independent genetic variants associated with a complex phenotype converge on intermediate genes, with a major role for the HLA. *PLoS genetics* **7**, e1002197 (2011).
- <sup>13</sup> Lieberman-Aiden, E. *et al.* Comprehensive mapping of long-range interactions reveals folding principles of the human genome. *Science (New York, N.Y.)* **326**, 289–93 (2009).

- <sup>14</sup> Visscher, P. M., Brown, M. a., McCarthy, M. I. & Yang, J. Five years of GWAS discovery. *American journal of human genetics* **90**, 7–24 (2012).
- <sup>15</sup> Weinreich, D. M., Delaney, N. F., Depristo, M. a. & Hartl, D. L. Darwinian evolution can follow only very few mutational paths to fitter proteins. *Science (New York, N.Y.)* **312**, 111–4 (2006).
- <sup>16</sup> Breen, M. S., Kemena, C., Vlasov, P. K., Notredame, C. & Kondrashov, F. a. Epistasis as the primary factor in molecular evolution. *Nature* **490**, 535–538 (2012).
- <sup>17</sup> Weir, B. S. Linkage disequilibrium and association mapping. *Annual review of genomics and human genetics* **9**, 129–42 (2008).
- <sup>18</sup> Hemani, G., Knott, S. & Haley, C. An Evolutionary Perspective on Epistasis and the Missing Heritability. *PLoS Genetics* **9**, e1003295 (2013).
- <sup>19</sup> Marchini, J., Donnelly, P. & Cardon, L. R. Genome-wide strategies for detecting multiple loci that influence complex diseases. *Nature Genetics* **37**, 413–417 (2005).
- <sup>20</sup> Lango Allen, H. *et al.* Hundreds of variants clustered in genomic loci and biological pathways affect human height. *Nature* **467**, 832–8 (2010).
- <sup>21</sup> Schadt, E. *et al.* Genetics of gene expression surveyed in maize, mouse and man. *Nature* **422**, 297–302 (2003).
- <sup>22</sup> Powell, J. E. *et al.* Congruence of Additive and Non-Additive Effects on Gene Expression Estimated from Pedigree and SNP Data. *PLoS Genetics* **9**, e1003502 (2013).
- <sup>23</sup> Powell, J. E. *et al.* The Brisbane Systems Genetics Study: genetical genomics meets complex trait genetics. *PloS one* **7**, e35430 (2012).
- <sup>24</sup> Preininger, M. *et al.* Blood-informative transcripts define nine common axes of peripheral blood gene expression. *PLoS genetics* **9**, e1003362 (2013).
- <sup>25</sup> Cockerham, C. C. An extension of the concept of partitioning hereditary variance for analysis of covariances among relatives when epistasis is present. *Genetics* **39**, 859–882 (1954).
- <sup>26</sup> Ho, T. H. *et al.* Muscleblind proteins regulate alternative splicing. *The EMBO journal* **23**, 3103–12 (2004).
- <sup>27</sup> Trynka, G. *et al.* Chromatin marks identify critical cell types for fine mapping complex trait variants. *Nature genetics* **45**, 124–30 (2013).
- <sup>28</sup> Hoffman, M., Buske, O., Wang, J. & Weng, Z. Unsupervised pattern discovery in human chromatin structure through genomic segmentation. *Nature Methods* **9**, 473–476 (2012).

- <sup>29</sup> Lan, X. *et al.* Integration of Hi-C and ChIP-seq data reveals distinct types of chromatin linkages. *Nucleic acids research* **40**, 7690–704 (2012).
- <sup>30</sup> Rieder, D., Trajanoski, Z. & McNally, J. G. Transcription factories. *Frontiers in genetics* **3**, 221 (2012).

## Supplementary Figures

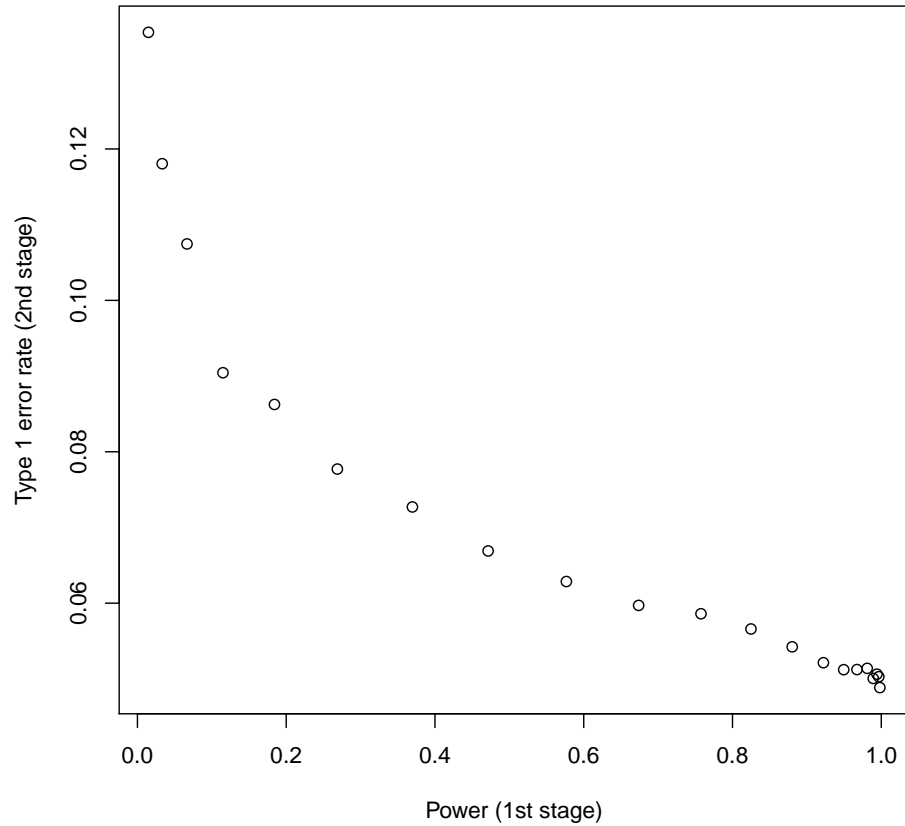


Figure S1: **Type 1 error rate of two stage design assuming a null model of one large additive effect and no epistasis** In stage 1 SNPs are tested for full genetic effects (8 d.f.) and those that surpass a threshold for multiple testing are then tested for significant interaction terms in stage 2. These interaction  $p$ -values are then adjusted (Bonferroni) for the total number of tests that passed stage 1. The type 1 error rate of this two stage design is dependent on the power, which is not known empirically.

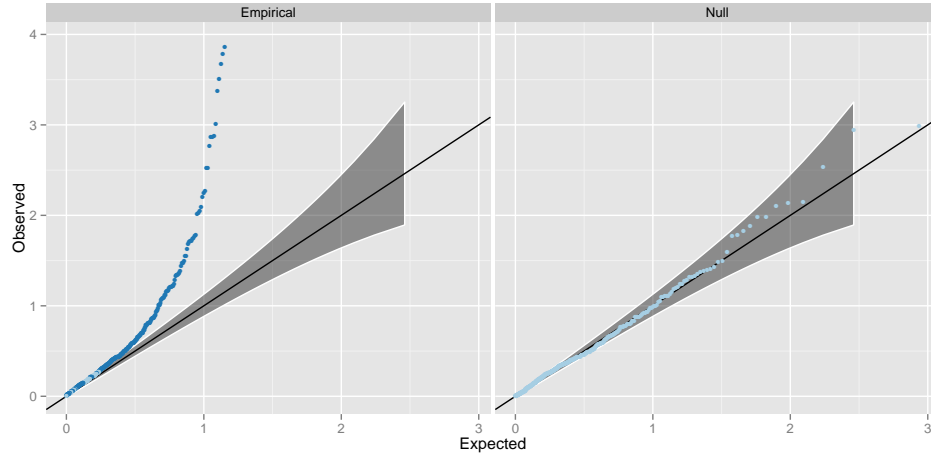


Figure S2: **Q-Q plots of interaction  $p$ -values from replication datasets, excluding the 30 points significant at the Bonferroni level** The right panel (Null) shows the interaction  $p$ -values from a meta analysis across two independent datasets on 434 SNP pairs where one SNP has a marginal effect. The left panel (Empirical) shows the interaction  $p$ -values from the 404 putative interactions that were not significant at the Bonferroni correction threshold. Dark blue points represent  $p$ -values that surpass the 2.5% FDR level, as in Figure 2.

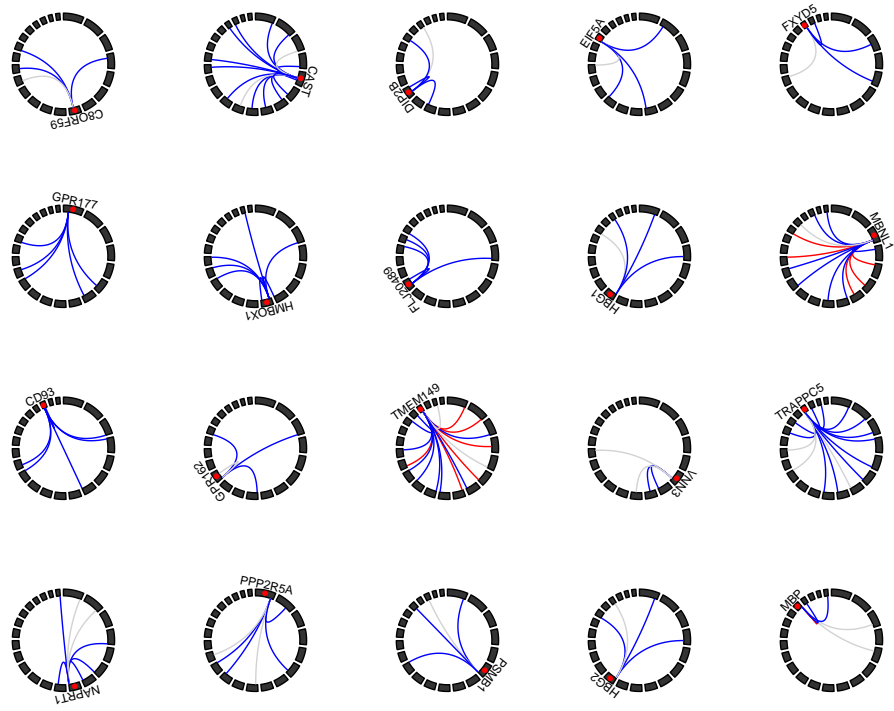
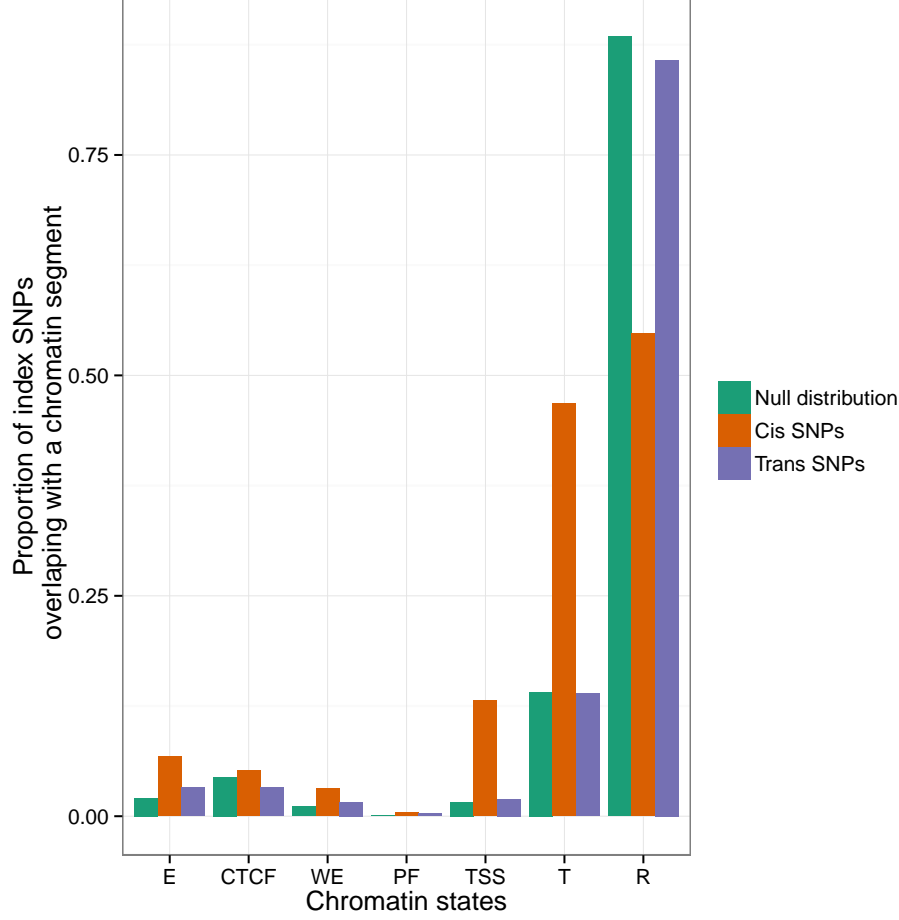
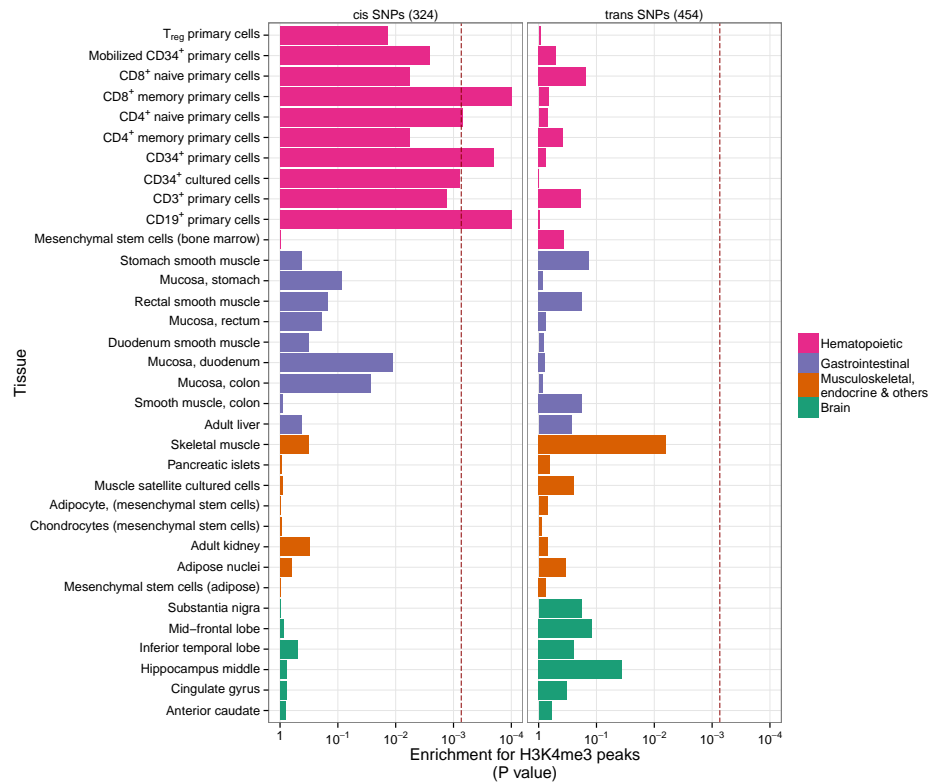


Figure S3: **Gene expression traits with four or more genetic interactions** Circle plots represent the genomic positions for SNPs (linking lines) and expression probes (red points). Chromosomes are represented by black blocks and ordered from 1 to 22 clockwise, starting from the top. Grey lines represent no evidence for replication, blue lines denote interactions that are outside the 97.5% confidence interval or the Q-Q plot (Figure 2), and red lines denote replication at the Bonferroni correction level. Most interactions are characterised as being *cis-trans* to the expression probe.



**Figure S4: Location of SNPs relative to genomic features** We used chromatin segmentation<sup>28</sup> as a method for labelling genomic features. All SNPs within 1Mb and  $r^2 > 0.8$  of each *cis*- and *trans*-SNP were taken to find which genomic features ( $x$ -axis) were covered by the SNPs that compose the 501 significant interactions. Green bars represent the proportion ( $y$ -axis) of the 528,509 SNPs used in the analysis that fall within the range of the different genomic features. There is enrichment for *cis*-acting SNPs (red bars) in promotor regions, but *trans*-acting SNPs (blue bars) are not enriched for genomic features. The labels on the  $x$ -axis are as follows: E = Predicted enhancer, CTCF = CTCF enriched element, WE = Predicted weak enhancer or open chromatin cis regulatory element, PF = Predicted promoter flanking region, TSS = Predicted promoter region including transcriptional start site, T = Predicted transcribed region, R = Predicted Repressed or Low Activity region





**Figure S5: Tissue specific enrichment of SNPs in transcriptionally active regions** The locations of transcriptional activity can be predicted by chromatin marks, assayed by H3K4me3.<sup>27</sup> Enrichment *p*-values are calculated using permutation analysis for 34 different cell types (*y*-axis) in four tissue types (Rows of boxes). The dotted red line denotes significance (Bonferroni correction for 34 cell types, *x*-axis). There is enrichment for *cis*-acting SNPs in Haematopoietic tissue types only. *Trans*-acting SNPs have no tissue specificity.

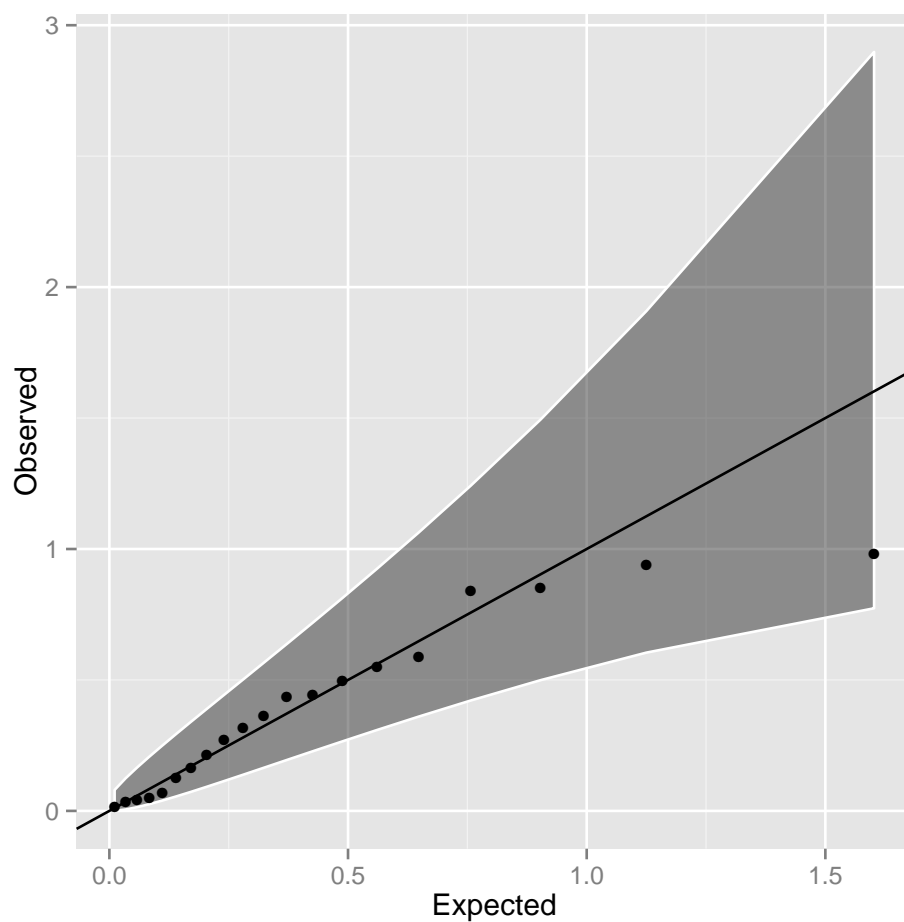


Figure S6: **Q-Q plot of interaction  $p$ -values in the CDHWB dataset**  
 Twenty of the 501 discovery SNP pairs passed filtering in the CDHWB dataset (mainly due to small sample size). There is no evidence for enrichment of interaction terms, most likely due to insufficient power given the limited sample size.

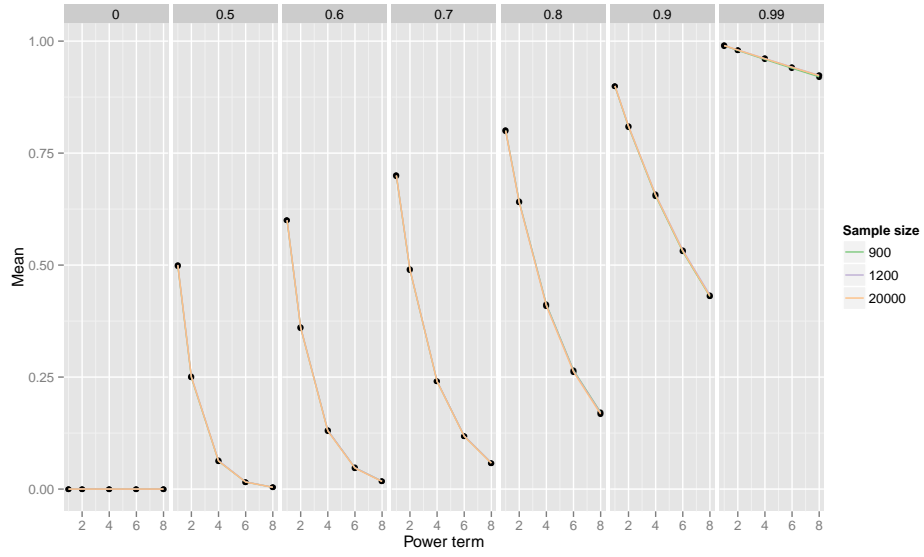
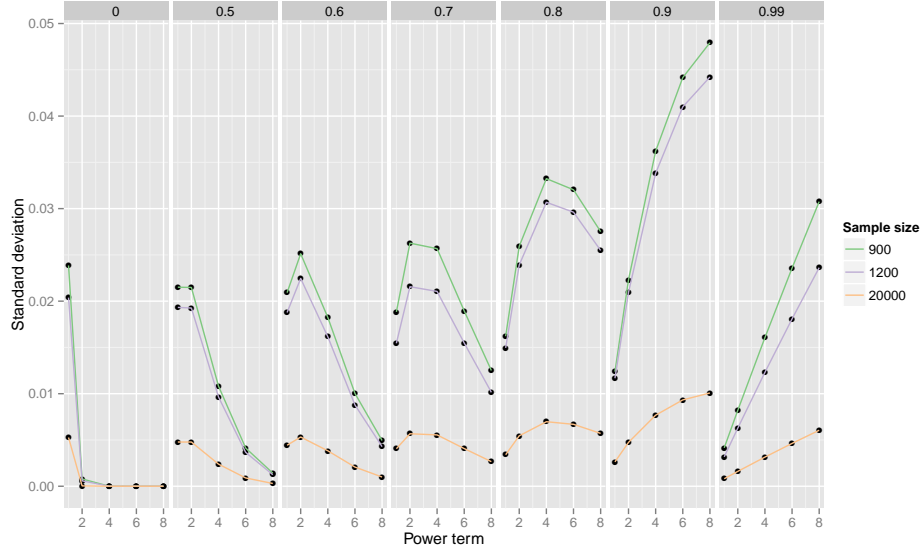


Figure S7: **Sampling mean for different power terms of population  $r$  values** Power of detection and replication of epistatic interactions depends not on  $r^2$  between causal variants and observed SNPs, but on  $r^4, r^6, r^8$ . For a given population value of LD  $r$  (columns of plots), plotted is the sample mean ( $y$ -axis) of  $\hat{r}$ ,  $\hat{r}^2$  (additive),  $\hat{r}^4$  (dominance,  $A \times A$ ),  $\hat{r}^6$  ( $A \times D$ ),  $\hat{r}^8$  ( $D \times D$ ) ( $x$ -axis) for different sample sizes (coloured lines). As true  $r$  reduces the statistical power to detect epistatic variants drops dramatically under the assumption that statistical power is proportional to higher moments of  $r$ .



**Figure S8: Sampling standard deviation for different power terms of population  $r$  values** Power of detection and replication of epistatic interactions depends not on  $r^2$  between causal variants and observed SNPs, but on  $r^4, r^6, r^8$ . For a given a population value of LD  $r$  (columns of plots), plotted is the sampling standard deviation ( $y$ -axis) of  $\hat{r}$ ,  $\hat{r}^2$  (additive),  $\hat{r}^4$  (dominance,  $A \times A$ ),  $\hat{r}^6$  ( $A \times D$ ),  $\hat{r}^8$  ( $D \times D$ ) ( $x$ -axis) for different sample sizes (coloured lines). As the power term of  $r$  increases the sampling variance also increases. Supposing that there is sufficiently high  $r^x$  in the discovery sample for detection of epistasis, the replication sample is less likely to have similarly high  $r^x$  as  $x$  increases, leading to an expectation of reduced replication rates.

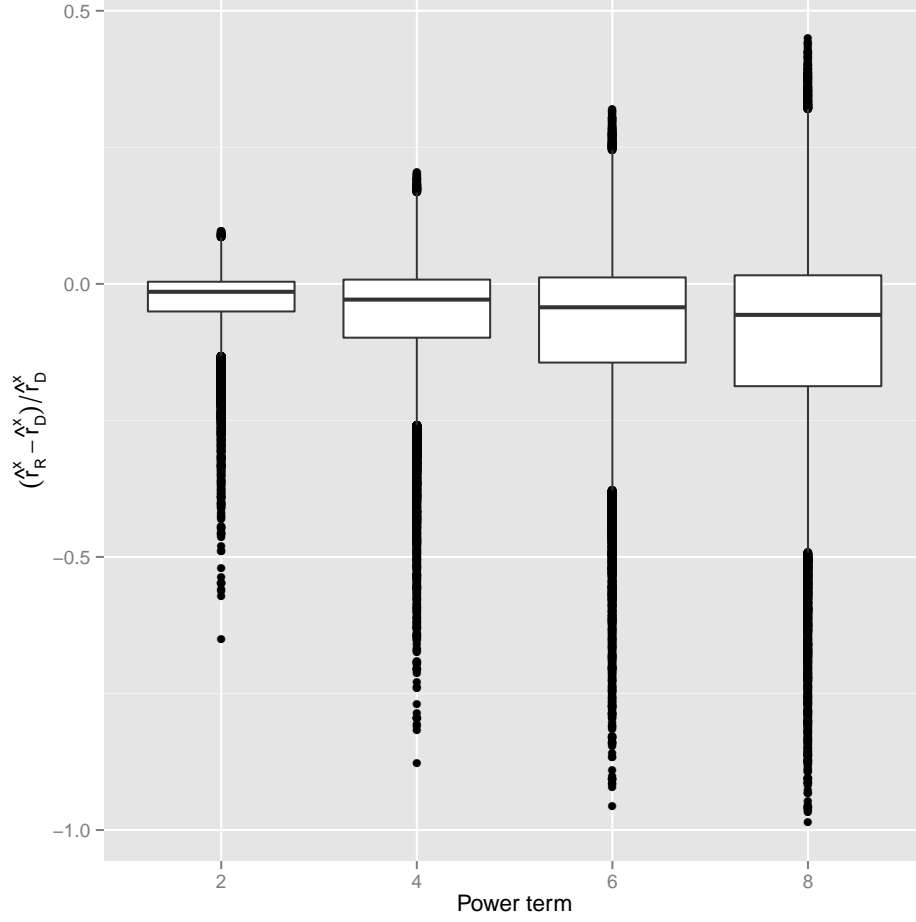


Figure S9: **Reduction in LD as estimated in replication data after ascertaining for high LD in discovery data** 100,000 “unobserved” causal variants (CVs) were tested for LD against a panel of 528,509 “observed” discovery markers (DMs). DM/CV pairs with LD  $r^2 > 0.9$  were then tested in an independent sample. Simulation results of the proportional decrease between discovery and replication datasets in LD ( $y$ -axis) of  $\hat{r}^2, \hat{r}^4, \hat{r}^6, \hat{r}^8$  ( $x$ -axis) are shown, where  $\hat{r}_D^x$  and  $\hat{r}_R^x$  are the sample LD measurements in the discovery and replication datasets, respectively. The average proportional decrease in the replication  $\hat{r}_R^x$  was 2.8%, 5.3%, 7.4% and 9.2% for  $x = 2, 4, 6$  and 8, respectively.

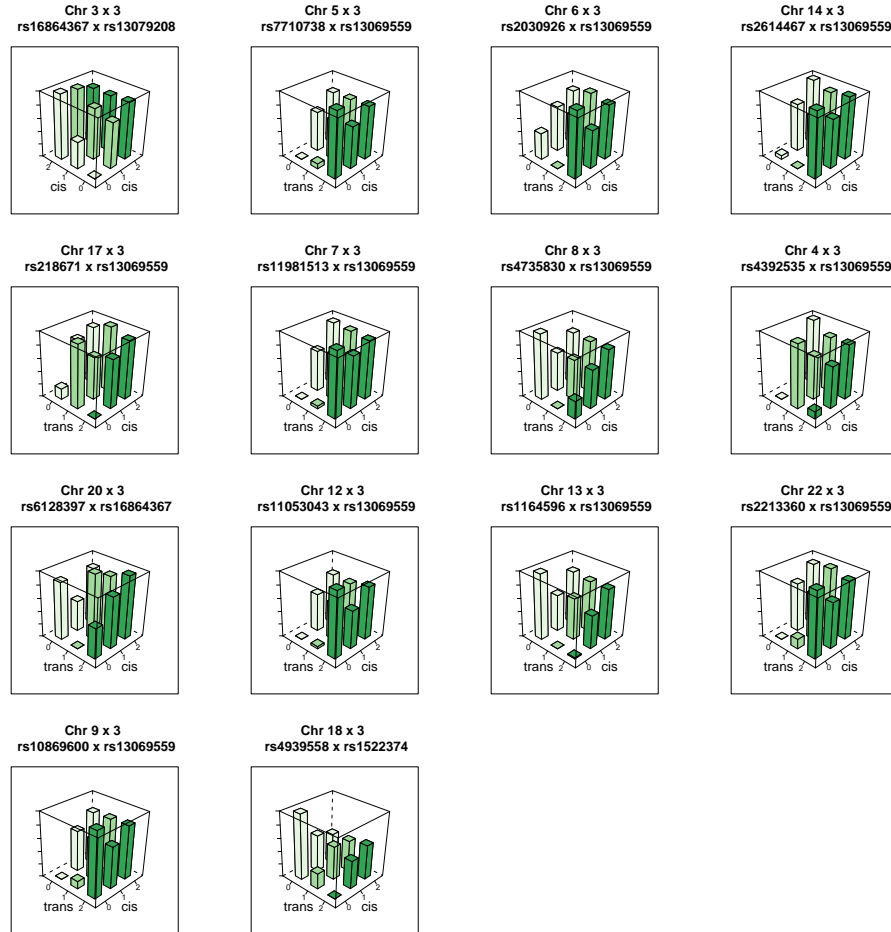


Figure S10: **Genotype-phenotype maps for 14 interactions influencing the expression of MBNL1** Each bar represents the mean phenotypic value for individuals in that genotype class. The rs13069559 SNP typically has a *cis*-additive decreasing effect on the expression of MBNL1, but in many of these interactions the *cis* effect is masked when the *trans* SNP is homozygous for the masking allele.

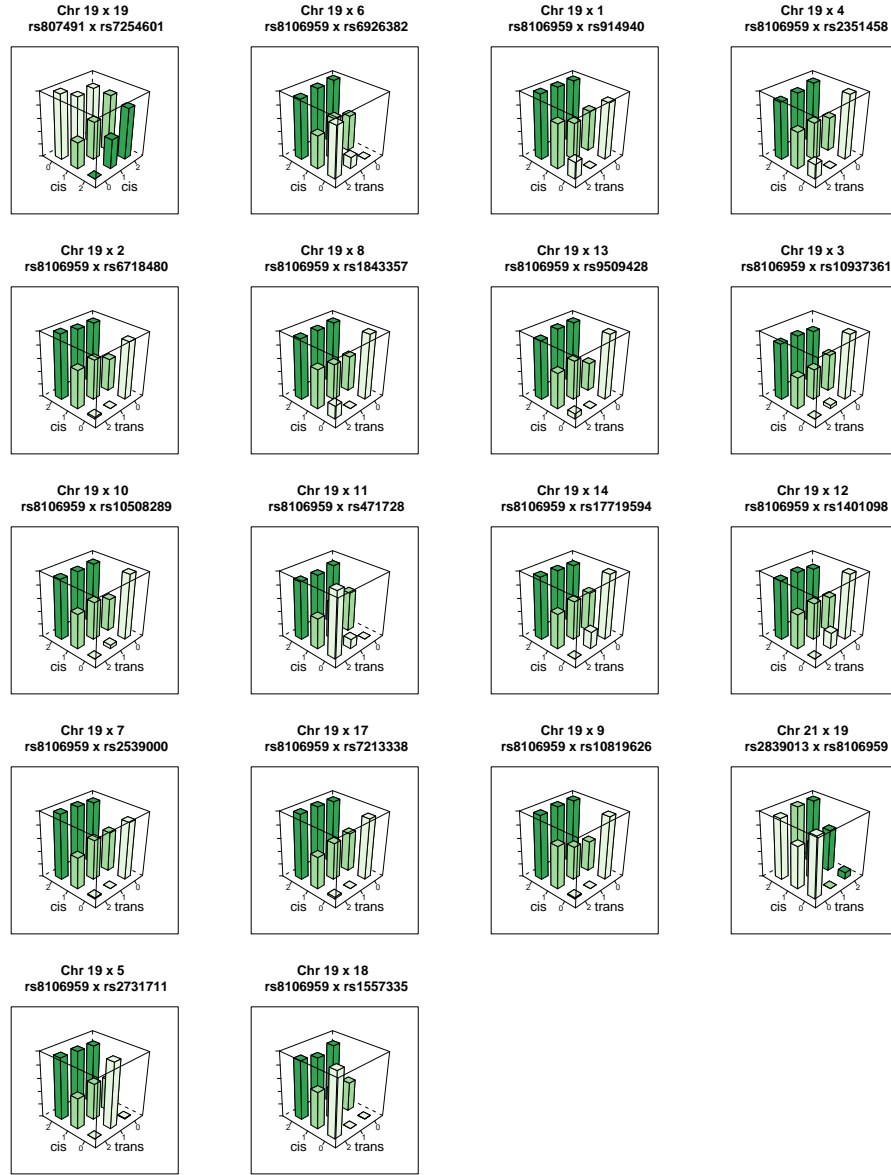


Figure S11: **Genotype-phenotype maps for 19 interactions influencing the expression of TMEM149** Each bar represents the mean phenotypic value for individuals in that genotype class. The rs13069559 SNP typically has a *cis*-additive decreasing effect on the expression of TMEM149, but in many of these interactions the *cis* effect is masked when the *trans* SNP is homozygous for the masking allele.

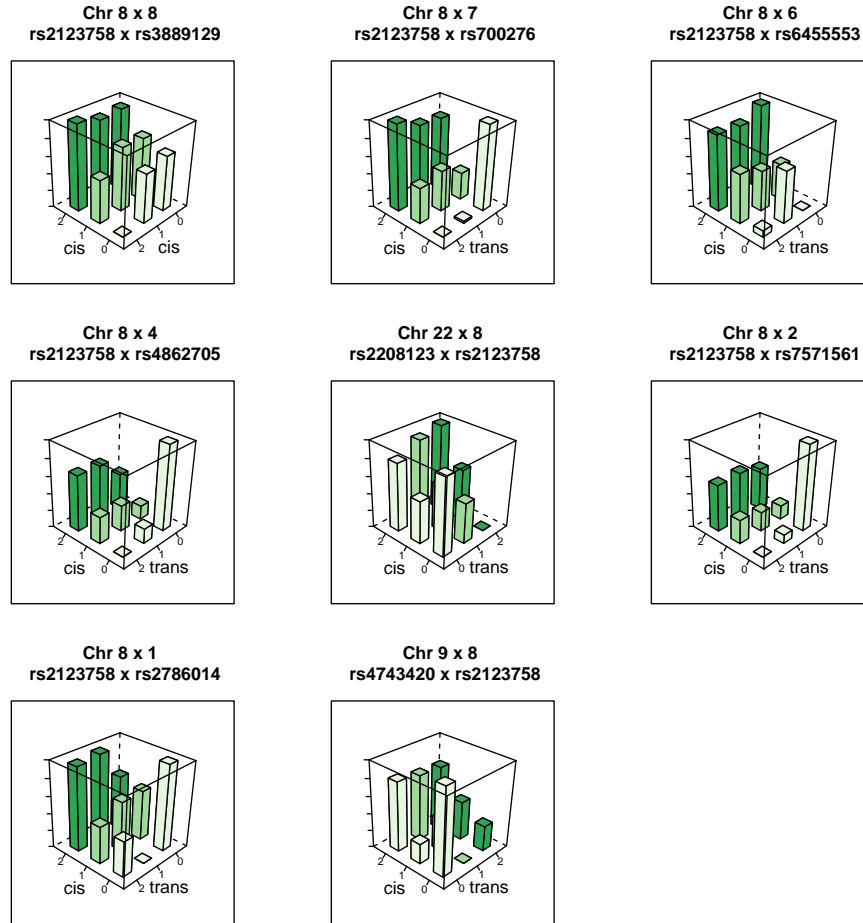


Figure S12: **Genotype-phenotype maps for 8 interactions influencing the expression of NAPRT1** Each bar represents the mean phenotypic value for individuals in that genotype class.



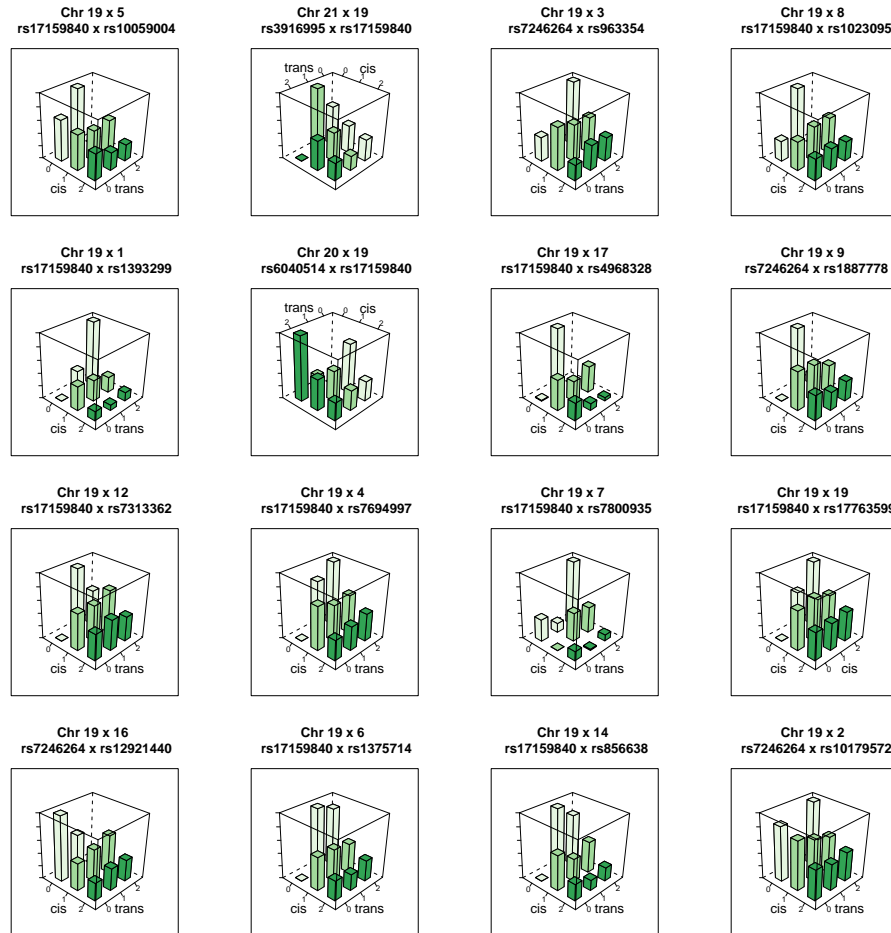


Figure S13: **Genotype-phenotype maps for 16 interactions influencing the expression of TRAPPC5** Each bar represents the mean phenotypic value for individuals in that genotype class.

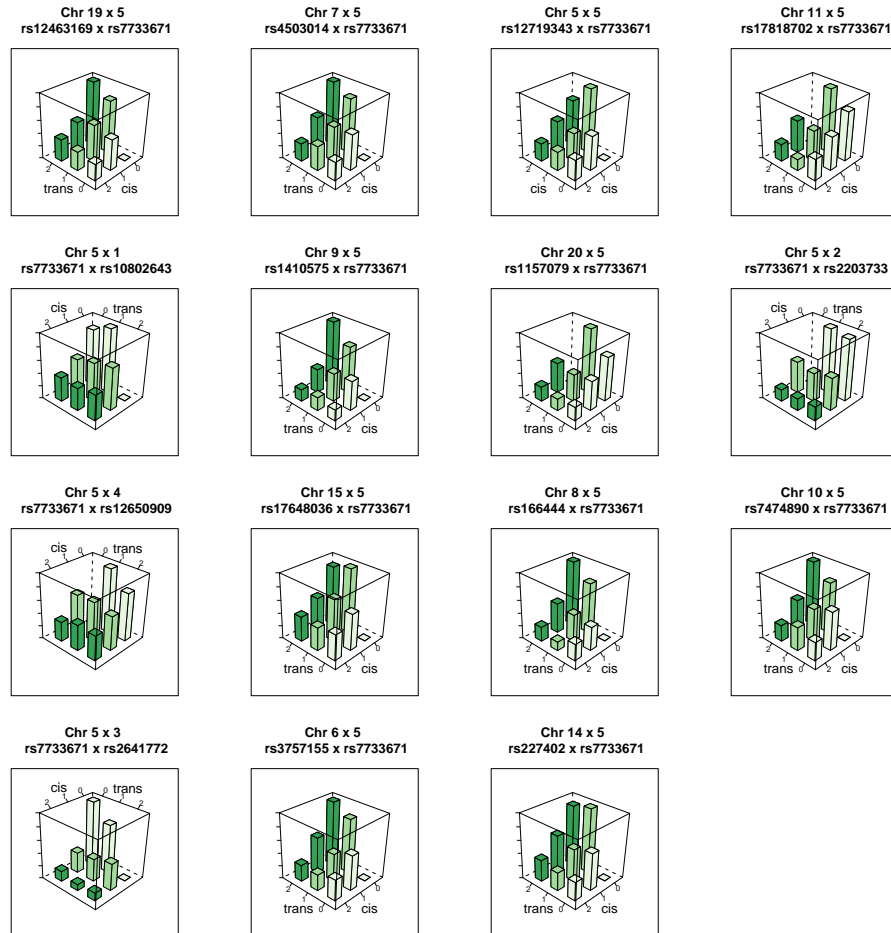
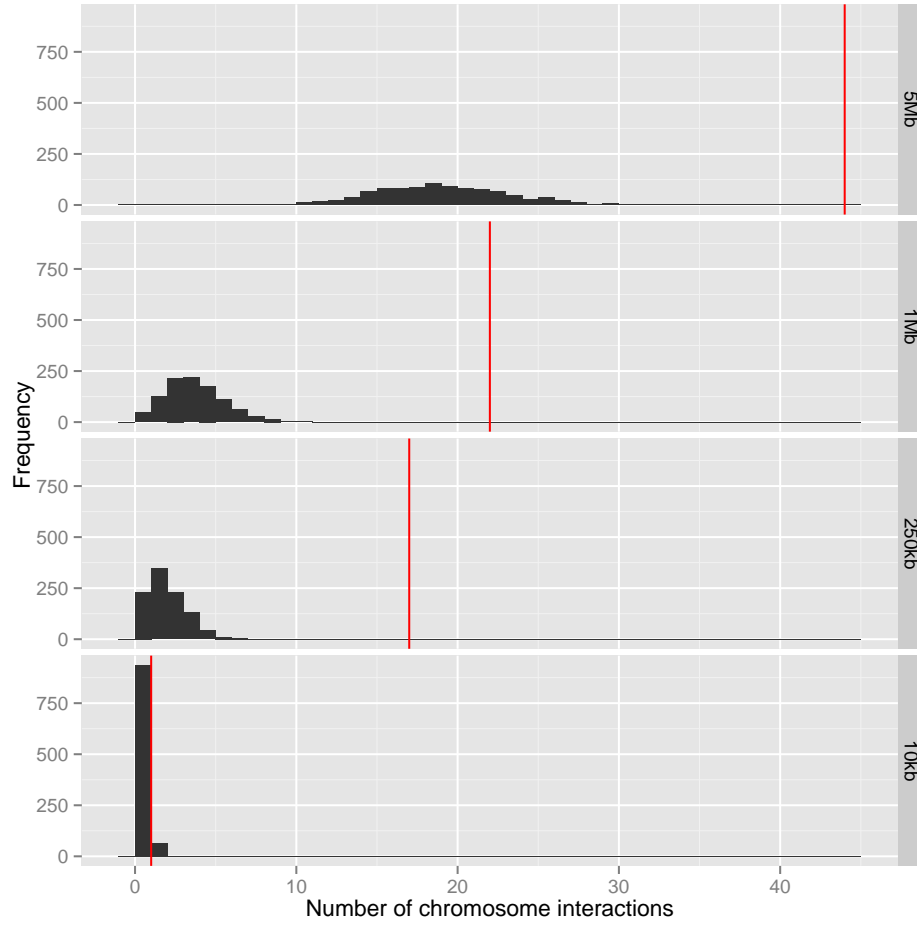


Figure S14: **Genotype-phenotype maps for 15 interactions influencing the expression of CAST** Each bar represents the mean phenotypic value for individuals in that genotype class.



**Figure S15: Number of overlaps between chromosome interactions and epistatic interactions** Interacting chromosome regions may be a possible mechanism underlying epistatic interactions. The number of epistatic interactions within 20kb, 500kb, 2Mb and 10Mb of known chromosome interacting regions are shown by red vertical lines. The histograms represent the null distribution based on random sampling of 1,000 datasets for each window size.

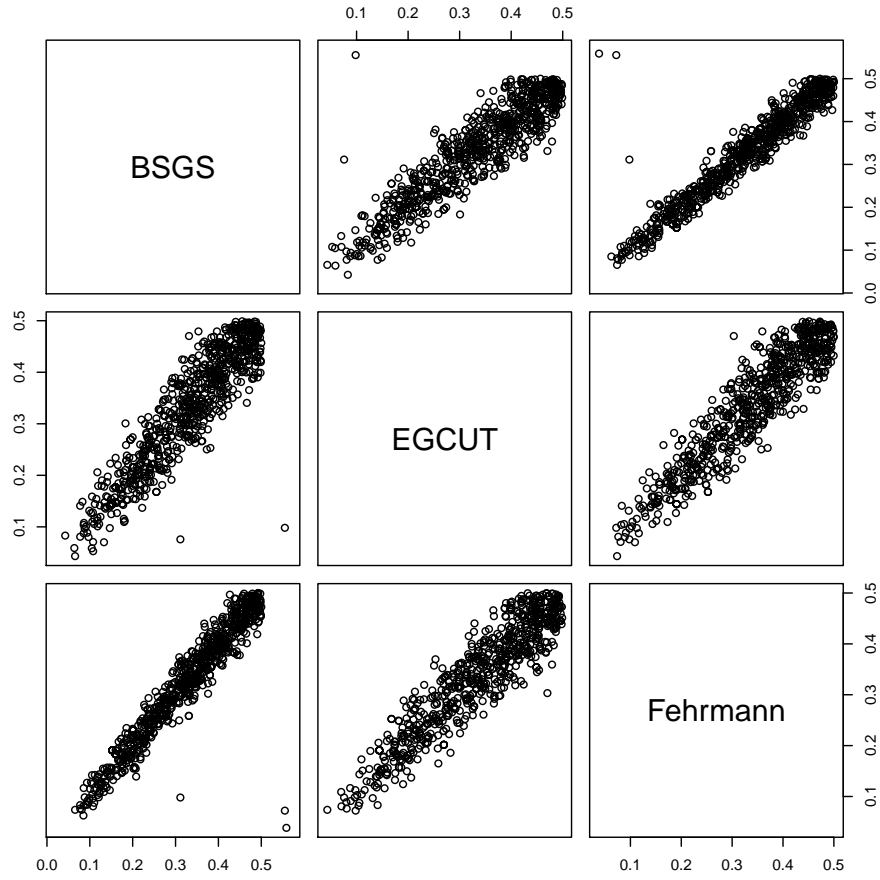
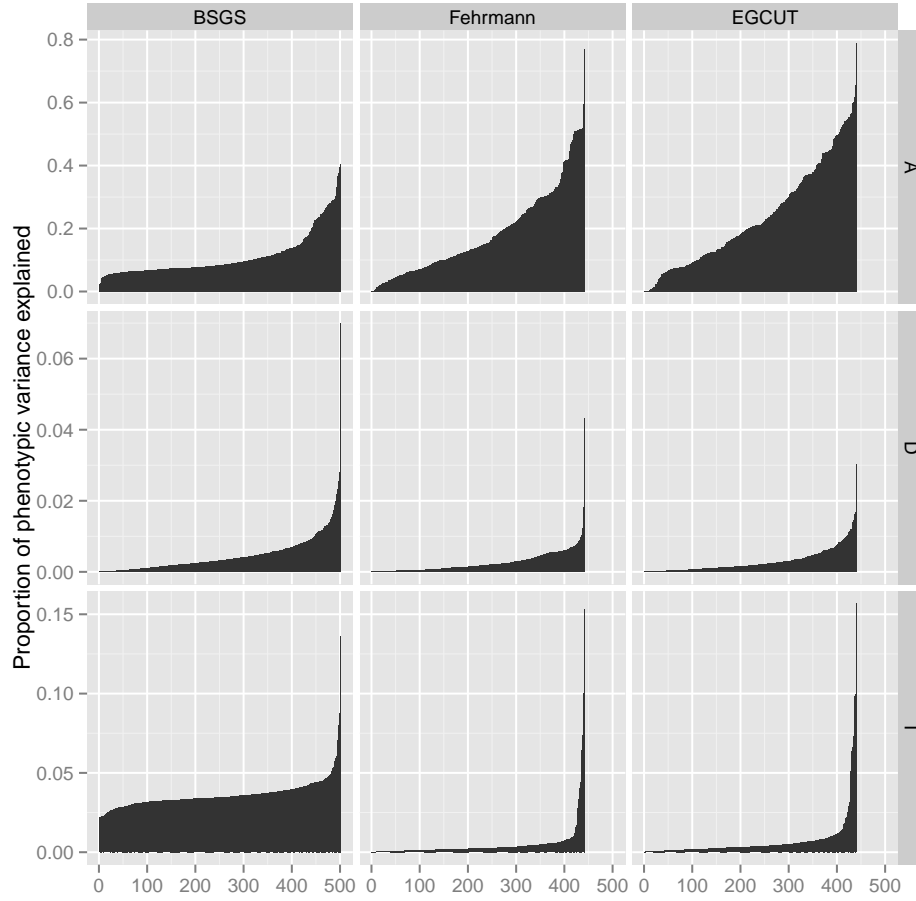


Figure S16: **Comparison of allele frequencies for 781 SNPs involved in genetic interactions across independent populations** Outliers were removed from the analysis as part of the filtering stage during replication.



**Figure S17: Comparison of variance explained by additive, dominant and epistatic effects from different cohorts** How does the estimated variance decomposition change in different cohorts? The proportion of the phenotypic variance that is additive (A), dominant (D), or epistatic (I) for each putative interaction is shown on the  $y$ -axis (Note: different scales for each row). BSGS has 501 interactions whereas Fehrmann and EGCUT have 434 ( $x$ -axis). The variance estimates in each plot are ordered from lowest additive to highest. This is done independently for each cohort to depict the distribution of estimated effects.

## Supplementary Tables



Gene ID <sup>a</sup>	Expression trait		SNP 1						SNP 2						Interaction statistic / $- \log_{10} p\text{-values}$		Distance / Mb
	Chr.	rs ID	Chr.	Pos /Mb/c	Association <sup>d</sup>	rs ID	Chr.	Pos /Mb/c	Association <sup>d</sup>	BSGS <sup>e</sup>	Fehrmann <sup>f</sup>	EGCUT <sup>g</sup>	Metas <sup>h</sup>				
C9ORF59	8	rs8051751	16	7188323		rs252669452	8	86102223	C9ORF59	5.79	1.39	0.18	0.87	29.369			
C9ORF72	9	rs101212902	9	27556780	C9ORF72	rs252669452	1	242029101		6.36	0.96	0.01	0.37				
CABD1	1	rs1261731064	10	4353908		rs7338725	1	227174210	CABD1	6.36	0.94	0.00	0.34				
CARD9	9	rs4266763	9	139289825	INPP5E	rs684040	1	82128660		5.81							
CARD9	9	rs4573661	11	6026661		rs4077515	9	139266496	INPP5E	6.61	0.09	0.86	0.42				
CAST	5	rs1157079	20	6778978		rs7733671	5	96000269	CAST	7.07	0.23	0.96	0.62				
ILMN-1712384	5	rs12463169	18	17321669		rs7733671	5	96000269	CAST	5.73	0.02	2.85	1.75				
ILMN-1712384	5	rs12599264	16	81840122		rs7733671	5	96000269	CAST	7.00							
ILMN-1712384	5	rs12719343	5	125369113		rs7733671	5	96000269	CAST		0.36	1.57	1.20				
ILMN-1712384	5	rs141010575	9	78255630		rs7733671	5	96000269	CAST	6.58	0.13	1.34	0.78				
ILMN-1712384	5	rs1466444	8	78392711		rs7733671	5	96000269	CAST	7.01	0.27	0.52	0.37				
ILMN-1712384	5	rs17648036	15	2731111		rs7733671	5	96000269	CAST	7.81	0.97	0.03	0.41				
ILMN-1712384	5	rs17818702	11	80107920		rs7733671	5	96000269	CAST	6.62	1.15	0.59	1.09				
ILMN-1712384	5	rs27402	14	70496867		rs7733671	5	96000269	CAST	6.12	0.11	0.01	0.01				
ILMN-1712384	5	rs2822124	21	15166804		rs7733671	5	96000269	CAST	6.87							
ILMN-1712384	5	rs3757155	6	136458593		rs7733671	5	96000269	CAST	7.24	0.07	0.33	0.12				
ILMN-1712384	5	rs4503014	7	31149140		rs7733671	5	96000269	CAST	5.88	0.92	1.56	1.72				
ILMN-1712384	5	rs4744890	17	59500078		rs7733671	5	96000269	CAST	6.74	0.12	0.23	0.23				
ILMN-1712384	5	rs7733671	5	96000269	CAST	rs10802643	1	238120177		7.42	0.75	0.78	0.93				
ILMN-1712384	5	rs7733671	5	96000269	CAST	rs12650909	4	170192890		7.42	0.23	0.78	0.50				
ILMN-1712384	5	rs7733671	5	96000269	CAST	rs2203733	2	224093101		6.07	0.22	0.87	0.54				
ILMN-1712384	5	rs7733671	5	96000269	CAST	rs2641772	3	195531841		6.93	0.19	0.26	0.15				
ILMN-16517005	11	rs772311	18	66175386		rs11032695	11	34447586	CAT	6.41	0.26	0.30	0.22				
ILMN-172208	11	rs2352108	19	17099980		rs541207	11	64125142	CDC8B	5.68	0.33	0.37	0.31				
ILMN-172208	11	rs694739	11	64097233	CDC8B	rs127171349	10	96989193	VAMP8	5.62	0.23	0.18	0.14				
ILMN-1784863	7	rs20811834	7	80280117		rs1254900	2	85816334		6.93	0.15	0.01	0.02				
ILMN-1800540	1	rs750801	11	76033374		rs67000168	1	207502534	CD55	5.09	0.08	0.03	0.02				
D9G3	20	rs1884655	20	23074375	D9G3	rs10255470	7	157182040		6.06	1.74	0.24	1.20				
D9G3	20	rs1884655	20	23074375	D9G3	rs4696726	4	7992632		5.71	0.13</						

Continued on next page



Table S1 – continued from previous page

Gene ID <sup>a</sup>	Expression trait	SNP 1		SNP 2		Interaction statistic / -log <sub>10</sub> p-values				Distance / Mb <sup>b</sup>				
		Chr.	rs ID	Pos/Mb <sup>c</sup>	Association <sup>d</sup>	Chr.	rs ID	Pos/Mb <sup>c</sup>	Association <sup>d</sup>					
CPVL	ILMN-1682928	7	rs2835998	21	39202070		rs245884	7	29185475	CPVL	5.55	0.19	0.03	0.04
CRPT	ILMN-1813256	2	rs2131290	4	188539908		rs1531133	7	46843651	CRPT	5.47	0.28	0.10	0.12
CRUS1	ILMN-1737685	20	rs6139887	20	5986234	CRUS1	rs1473927	5	62406408		6.18	0.10	0.36	0.15
CS1B	ILMN-1761797	21	rs6979356	21	43230974		rs3761385	21	45196355		11.99	25.20	16.72	42.27
CTNNA1	ILMN-1804854	5	rs924943	18	69000505		rs176382	5	138226707	CTNNA1	5.74	0.02	0.41	0.11
CTSC	ILMN-1696347	11	rs2457684	11	88139983	CTSC	rs7079264	10	10679892		5.67	0.92	0.74	0.03
CTSC	ILMN-1696347	11	rs7532236	22	26250645		rs7128352	11	88087357	CTSC	5.84	0.49	0.73	0.73
CTSC	ILMN-2242463	11	rs7930237	21	88117962		rs156895	11	88077479		7.16	18.76	15.06	33.53
CWF19L1	ILMN-1651886	10	rs7108734	11	11450027		rs12784396	10	102027407	CWF19L1	5.42	0.21	0.01	0.03
CYBRD1	ILMN-1712305	4	rs2592948	4	129994690		rs888427	2	172366120	CYBRD1	5.89	0.23	0.53	0.34
CYBRD1	ILMN-1712305	2	rs7852475	9	140698856		rs888427	2	172366120	CYBRD1	5.68	0.20	0.02	0.04
CYBRD1	ILMN-2087692	2	rs11257679	10	12318284		rs888427	2	172366120	CYBRD1	5.81	0.39	1.87	1.47
CYBRD1	ILMN-2087692	2	rs6137908	20	23344590		rs888427	2	172366120	CYBRD1	5.53	0.05	0.83	0.36
CYP27A1	ILMN-1704985	2	rs888427	20	172366120	CYBRD1	rs7591849	2	160112881	CYP27A1	5.85	0.87	0.10	0.44
CYP27A1	ILMN-1704985	2	rs6021982	20	36571928		rs933994	2	219650616	CYP27A1	5.42	0.29	0.86	0.60
DAB2	ILMN-2128428	5	rs7778910	17	110451383		rs933994	2	219650616	DAB2	5.44	0.48	0.41	0.44
DDT	ILMN-1811648	17	rs9900173	17	43111688	DDT	rs1343244	9	82076988		5.12	0.00	0.58	0.14
DDT	ILMN-1690982	22	rs9760102	22	24248761		rs275341	3	187475208		5.62	0.64	0.25	0.42
DDX58	ILMN-1797001	9	rs4537097	11	125962645	COQ10A	rs7042042	7	32451144		5.31	0.61	0.29	0.44
DEM1	ILMN-1783996	1	rs10120023	9	137810259		rs10120023	9	137810259	COQ10A	5.37	0.08	0.41	0.16
DEM1	ILMN-1733998	1	rs12363827	13	106703727		rs7566044	2	169960422	DHSR9	6.39	0.77	0.02	0.58
DHSR9	ILMN-1733998	2	rs1511956	12	89468283		rs7566044	2	169960422	DHSR9	6.00	0.06	1.17	0.98
DHSR9	ILMN-2384181	2	rs1528529	12	147132505		rs2161037	2	169893419	DHSR9	6.48	0.37	0.34	0.32
DHSR9	ILMN-2384181	2	rs2831914	21	29959453		rs2161037	2	169893419	DHSR9	5.51	0.88	0.04	0.37
DHSR9	ILMN-2384181	4	rs7661304	4	18776631		rs1169322	12	50610976	LASS5	7.64	0.05	0.11	0.10
DIP2B	ILMN-1755589	12	rs11080134	17	29161503	LASS5	rs2872008	7	153134888	LASS5	4.65	0.32	0.05	0.10
DIP2B	ILMN-1755589	12	rs1169335	12	50636364		rs334859	12	50730458		4.87	0.30	0.58	0.19
DIP2B	ILMN-1755589	12	rs3383853	19	41711815	LASS5	rs184654	8	16971140	LASS5	5.31	0.38	0.22	0.19
DIP2B	ILMN-1755589	12	rs73134595	12	50730458	LASS5	rs1808634	10	115214154	LASS5	4.40	0.37	0.09	0.02
DIP2B	ILMN-1755589	12	rs7312252	12	50744171	LASS5	rs4532958	8	115214154	LASS5	5.03	0.09	0.02	0.01
DIP2B	ILMN-1755589	12	rs871257	12	117994348		rs12427378	12	51074199	DNABJB6	5.92	0.48	0.23	1.45
DNABJB6	ILMN-1793770	7	rs2288842	15	157216093		rs3775539	7	157163614	DNABJB6	5.79	0.23	1.45	0.97
DPH3	ILMN-2349610	3	rs12232308	15	93400954	ECGF1	rs1566972	3	16320360	DPH3	6.17	1.58	0.27	1.12
ECGF1	ILMN-2109708	22	rs14323491	22	50971266		rs4891884	18	64004670	DPH3	4.81	0.15	1.18	0.70
ECGF1	ILMN-1671568	1	rs4324091	22	241911027		rs11206043	1	53402552	ECGF1	6.19	0.22	0.35	0.22
ECGF1	ILMN-1671568	1	rs5092637	22	17675900		rs11206043	1	53402552	ECGF1	5.58	0.64	0.16	0.35
ECGF1	ILMN-1720083	15	rs5092637	22	17675900		rs1043166	15	42192040	ECGF1	6.98	0.90	0.47	0.79
EIF2B2	ILMN-1719380	14	rs6567288	18	60218334		rs1269096	14	99603119	EIF2B2	5.56	0.23	0.11	0.10
EIF2B2	ILMN-1704522	17	rs7216490	17	7221707	EIF5A	rs1754556	14	7550340	EIF2B2	5.44	0.56	0.08	0.24
EIF5A	ILMN-1794522	17	rs7216490	17	7221707	EIF5A	rs1553474	2	49359676	EIF2B2	5.55	0.28	0.05	0.41
EIF5A	ILMN-1745452	17	rs7216490	17	7221707	EIF5A	rs1553474	2	49359676	EIF2B2	5.55	0.28	0.05	0.41
EIF5A	ILMN-1794522	17	rs7216490	17	7221707	EIF5A	rs4471434	11	126387391	EIF2B2	5.52	0.05	1.12	0.53
EMR2	ILMN-2353633	19	rs2827076	21	23196249		rs9305048	19	14879034	EMR2	6.36	0.08	0.05	0.02
EMR2	ILMN-2353633	19	rs6132112	20	18761714		rs9305048	19	14879034	EMR2	6.51	0.36	0.04	0.11
EMR2	ILMN-2353633	19	rs9405048	19	14879034		rs3007765	13	102480759	EMR2	5.56	0.45	0.40	0.41
EMR2	ILMN-1709237	8	rs1107764	11	12790396	EMR2	rs3007765	13	102480759	EMR2	6.03	0.20	0.58	0.35
EPHX2	ILMN-1731001	8	rs10894861	11	13461176		rs13269963	13	102480759	EPHX2	5.70	0.20	0.58	0.35
EPHX2	ILMN-1731001	8	rs5766218	22	45337329		rs12115088	8	578752	EPHX2	6.11	0.25	1.20	0.81
EPHX2	ILMN-1731001	8	rs726145	18	31187910		rs12115088	8	578752	EPHX2	5.65	0.29	0.04	0.08
ERICH1	ILMN-2104696	5	rs4735895	8	600729	ERICH1	rs1517297	4	189786760	ERICH1	5.63	0.67	1.03	1.06
ERICH1	ILMN-2104696	5	rs187076	10	55228462		rs12188164	5	4928236	ERICH1	6.83	0.74	0.19	0.44
EXOC3	ILMN-1789419	5	rs1560104	16	12708208		rs344363	16	1972548	EXOC3	5.61	0.38	1.38	0.44
FAHD1	ILMN-2246661	9	rs12580388	12	129591144		rs10120023	9	137810259	FAHD1	6.33	0.27	0.30	0.23
FCN1	ILMN-1668063	12	rs12580388	12	129591144		rs10120023	9	137810259	FAHD1	6.33	0.27	0.30	0.23

Continued on next page

Table S1 – continued from previous page

Gene ID <sup>a</sup>	Probe ID <sup>b</sup>	Chr.	rs ID	Chr.	SNP 1	Pos/Mb <sup>c</sup>	Association <sup>d</sup>	rs ID	Chr.	SNP 2	Pos/Mb <sup>c</sup>	Association <sup>d</sup>	BSGS <sup>e</sup>	Interaction statistic <sup>f</sup>	EGCUT <sup>g</sup>	− log <sub>10</sub> <i>p</i> -value	Distance / Mb <sup>h</sup>
FE2Z	ILMN_1739586	2	rs2356400	19	44321776	19		rs13406184	2	36791226	FE2Z	FE2Z	5.78	0.14	0.33	0.16	
FE2Z	ILMN_1739586	2	rs969010	4	159963132	4		rs11691600	6	36810133	FE2Z	FE2Z	6.59	0.14	0.28	0.14	
FGD2	ILMN_2115005	6	rs4803848	19	46203050	19		rs831486	6	37001267	FGD2	FGD2	5.69	0.12	0.25	0.11	
FGD2	ILMN_2115005	6	rs902634	12	133943531	12		rs351498	6	36999652	FGD2	FGD2	5.49	1.20	0.11	0.66	68.867
FLJ20489	ILMN_1761073	12	rs17036706	12	177036706	12	FLJ20489	rs831486	6	41699526	FLJ20489	FLJ20489	5.81	0.06	0.70	0.29	
FLJ20489	ILMN_1761073	12	rs17036706	12	177036706	12		rs3782908	12	48169526	FLJ20489	FLJ20489	5.79	0.19	0.13	0.04	
FLJ20489	ILMN_1778144	12	rs7021190	15	70921190	15		rs3782908	12	48169526	FLJ20489	FLJ20489	5.79	0.19	0.13	0.04	
FLJ20489	ILMN_1778144	12	rs4984400	12	97033126	12		rs3782908	12	48169526	FLJ20489	FLJ20489	6.04	0.31	0.47	0.36	
FLJ20489	ILMN_1778144	12	rs7204135	16	50626195	12		rs3782908	12	48169526	FLJ20489	FLJ20489	6.00	0.38	0.17	0.21	
FLJ20489	ILMN_1763663	16	rs9325634	21	43818790	16		rs3782908	12	50116594	FLJ20489	FLJ20489	6.04	0.14	0.95	0.53	
FLJ43093	ILMN_2123450	6	rs6906101	14	107276627	6	FLJ43093	rs6906101	6	36676710	FLJ43093	FLJ43093	5.48	0.39	0.06	0.13	3.962
FLJ43093	ILMN_2123450	6	rs8980638	17	80890638	17		rs9892064	17	808297903	FLJ43093	FLJ43093	5.44	0.00	0.64	0.18	0.063
FN3KRP	ILMN_1762333	17	rs8980638	17	80890638	17		rs9892064	17	808297903	FN3KRP	FUCA1	6.41	0.01	0.30	0.06	
FXYD5	ILMN_1762333	17	rs4971478	19	356952921	2		rs8281878	13	98328559	FXYD5	FXYD5	3.70	0.09	0.41	0.17	
FXYD5	ILMN_2309848	19	rs1633921	19	356952921	19		rs7781878	13	98328559	FXYD5	FXYD5	3.70	0.09	0.41	0.17	
FXYD5	ILMN_2309848	19	rs17398183	20	55609148	19	FXYD5	rs11739594	3	35660450	FXYD5	FXYD5	6.58	0.03	0.48	0.15	
FXYD5	ILMN_2309848	19	rs2285515	19	35660450	19	FXYD5	rs13067700	3	95331048	FXYD5	FXYD5	5.70	0.07	0.17	0.05	
FXYD5	ILMN_2309848	19	rs2285515	19	35660450	19	FXYD5	rs17036504	2	47567329	FXYD5	FXYD5	6.00	0.09	0.09	0.51	0.22
G3BP2	ILMN_2309848	4	rs10230232	7	29390239	4		rs1553985	4	76574604	G3BP2	G3BP2	6.10	0.28	0.08	0.37	0.14
GAA	ILMN_2410783	17	rs11150847	17	78153130	17	GAA	rs12602462	17	78146016	GAA	GAA	13.91	19.98	12.99	32.60	0.007
GAA	ILMN_2410783	17	rs8068856	17	78100731	17		rs10902506	12	132678089	GAA	GAA	5.65	0.11	0.39	0.17	
GAPT	ILMN_1675191	5	rs10070522	5	57786110	5	GAPT	rs7605821	2	2356955228	GAPT	GAPT	5.05	0.11	0.78	0.28	
GAPT	ILMN_1675191	5	rs7082031	10	128038717	10		rs10070522	5	57786110	GAPT	GAPT	5.72	0.26	0.11	0.11	
GATS	ILMN_1699631	7	rs1147447	14	66460742	7	GATS	rs29505020	7	99827148	GATS	GATS	5.47	0.83	0.63	0.87	
GATS	ILMN_1699631	7	rs2452566	20	35056572	20		rs29505020	7	99827148	GATS	GATS	6.22	0.42	0.35	0.33	
GDPD3	ILMN_1774901	16	rs8090624	16	30102802	16	GDPD3	rs2197465	14	48572632	GDPD3	GDPD3	6.57	0.38	0.35	0.24	
GDPD3	ILMN_1774901	16	rs7204270	16	30156963	16	GDPD3	rs1015111	4	128972357	GDPD3	GDPD3	5.86	0.55	0.09	0.24	
GDPD3	ILMN_1774901	16	rs7204270	16	30156963	16		rs75777293	4	128972357	GDPD3	GDPD3	5.78	0.02	0.45	0.13	
GNLY	ILMN_1790692	2	rs145072	13	110899955	2		rs7960552	12	111164237	GNLY	GNLY	5.72	0.36	0.46	0.39	
GNLY	ILMN_3239426	12	rs17198646	16	26084476	16		rs7960552	12	111164237	GNLY	GNLY	5.07	0.25	0.06	0.07	
GNLY	ILMN_3239426	12	rs1860563	16	6478898	16		rs2707210	12	6902002	GNLY	GNLY	5.47	0.25	0.06	0.07	
GPR162	ILMN_1730816	12	rs2272500	12	79685913	12		rs2707210	12	6902002	GPR162	GPR162	5.07	0.25	0.06	0.07	
GPR162	ILMN_1730816	12	rs2272500	12	79685913	12		rs2707210	12	6902002	GPR162	GPR162	5.07	0.25	0.06	0.07	
GPR162	ILMN_1730816	12	rs2707210	12	6902002	12		rs2707210	12	6902002	GPR162	GPR162	5.47	0.25	0.06	0.07	
GPR177	ILMN_1660549	1	rs11057383	12	124369421	12		rs9827054	3	188880113	GPR177	GPR177	6.21	0.96	0.06	0.44	
GPR177	ILMN_1660549	1	rs12527241	6	120468039	6		rs9827054	3	188880113	GPR177	GPR177	5.46	0.72	0.67	0.81	
GPR177	ILMN_1660549	1	rs12532999	1	127939793	1		rs12065581	1	68732819	GPR177	GPR177	5.76	0.79	1.43	1.50	
GPR177	ILMN_1660549	1	rs125613	16	11169683	1		rs12065581	1	68732819	GPR177	GPR177	5.43	0.79	1.43	1.50	
GPR177	ILMN_1660549	1	rs9575097	13	82986268	13		rs12065581	1	68732819	GPR177	GPR177	6.04	0.95	0.21	0.60	
GPR177	ILMN_1660549	1	rs6566699	18	70506011	1		rs12065581	1	68732819	GPR177	GPR177	5.86	0.24	0.34	0.23	
GPR177	ILMN_2283325	1	rs5929446	3	171399321	3		rs12065581	1	68732819	GPR177	GPR177	6.50	0.01	0.24	0.04	
GSDMB	ILMN_2347193	17	rs11557467	17	38028634	15	GSDMB	rs4965745	15	101508261	GSDMB	GSDMB	5.88	0.68	0.20	0.41	
GSTM1	ILMN_2391861	1	rs12244673	10	53192833	1		rs11101992	1	110266754	GSTM1	GSTM1	6.11	0.27	1.14	0.79	
GSTM1	ILMN_2391861	1	rs1547574	13	83344527	1		rs11101992	1	110266754	GSTM1	GSTM1	5.91	0.27	1.14	0.79	
GSTM2	ILMN_2201580	1	rs6432807	1	96139560	1		rs3754446	1	110253241	GSTM2	GSTM1	6.77	0.66	0.66	0.65	
H1FO	ILMN_1757467	22	rs139898	22	38399979	15		rs4533353	15	85877017	H1FO	H1FO	6.36	0.52	0.27	0.31	0.23
H1FO	ILMN_1757467	22	rs139898	22	38399979	15		rs6497007	17	15932546	H1FO	H1FO	6.52	0.40	0.25	0.48	0.32
H1FO	ILMN_1757467	22	rs139898	22	38399979	15		rs9885949	21	19532546	H1FO	H1FO	5.40	0.25	0.48	0.32	
H1FO	ILMN_1757467	22	rs139898	22	38399979	15		rs2855039	1	5271671	H1FO	H1FO	5.98	0.10	0.46	0.19	
H1FO	ILMN_1757467	22	rs139898	22	38399979	15		rs2855039	1	5271671	H1FO	H1FO	5.98	0.10	0.46	0.19	
HBG1	ILMN_1796678	11	rs12075066	11	35723407	11		rs12042181	1	213088494	HBG1	HBG2	6.78	0.08	0.52	0.21	
HBG1	ILMN_1796678	11	rs2855039	11	5271671	11	HBG2	rs12042181	1	213088494	HBG1	HBG2	6.78	0.08	0.52	0.21	
HBG1	ILMN_1796678	11	rs2855039	11	5271671	11	HBG2	rs12042181	1	213088494	HBG1	HBG2	6.78	0.08	0.52	0.21	
HBG1	ILMN_1796678	11	rs2855039	11	5271671	11	HBG2	rs12042181	1	213088494	HBG1	HBG2	6.78	0.08	0.52	0.21	
HBG1	ILMN_1796678	11	rs2855039	11	5271671	11	HBG2	rs12042181	1	213088494	HBG1	HBG2	6.78	0.08	0.52	0.21	
HBG1	ILMN_1796678	11	rs2855039	11	5271671	11	HBG2	rs12042181	1	213088494	HBG1	HBG2	6.78	0.08	0.52	0.21	
HBG1	ILMN_1796678	11	rs2855039	11	5271671	11	HBG2	rs12042181	1	213088494	HBG1	HBG2	6.78	0.08	0.52	0.21	
HBG1	ILMN_1796678	11	rs2855039	11	5271671	11	HBG2	rs12042181	1	213088494	HBG1	HBG2	6.78	0.08	0.52	0.21	
HBG1	ILMN_1796678	11	rs2855039	11	5271671	11	HBG2	rs12042181	1	213088494	HBG1	HBG2	6.78	0.08	0.52	0.21	
HBG1	ILMN_1796678	11	rs2855039	11	5271671	11	HBG2	rs12042181	1	213088494	HBG1	HBG2	6.78	0.08	0.52	0.21	
HBG1	ILMN_1796678	11	rs2855039	11	5271671	11	HBG2	rs12042181	1	213088494	HBG1	HBG2	6.78	0.08	0.52	0.21	
HBG1	ILMN_1796678	11	rs2855039	11	5271671	11	HBG2	rs12042181	1	213088494	HBG1	HBG2	6.78	0.08	0.52	0.21	
HBG1	ILMN_1796678	11	rs2855039	11	5271671	11	HBG2	rs12042181	1	213088494	HBG1	HBG2	6.78	0.08	0.52	0.21	
HBG1	ILMN_1796678	11	rs2855039	11	5271671	11	HBG2	rs12042181	1	213088494	HBG1	HBG2	6.78	0.08	0.52	0.21	
HBG1	ILMN_1796678	11	rs2855039	11	5271671	11	HBG2	rs12042181	1	213088494	HBG1	HBG2	6.78	0.08	0.52	0.21	
HBG1	ILMN_1796678	11	rs2855039	11	5271671	11	HBG2	rs12042181	1	213088494	HBG1	HBG2	6.78	0.08	0.52	0.21	
HBG1	ILMN_1796678	11	rs2855039	11	5271671	11	HBG2	rs12042181	1	213088494	HBG1	HBG2	6.78	0.08	0.52	0.21	
HBG1	ILMN_1796678	11	rs2855039	11	5271671	11	HBG2	rs12042181	1	213088494	HBG1	HBG2	6.78	0.08	0.52	0.21	
HBG1	ILMN_1796678	11	rs2855039	11	5271671	11	HBG2	rs12042181	1	213088494	HBG1	HBG2	6.78	0.08	0.52	0.21	
HBG1	ILMN_1796678	11	rs2855039	11	5271671	11	HBG2	rs12042181	1	213088494	HBG1	HBG2	6.78	0.08	0.52	0.21	
HBG1	ILMN_1796678	11	rs2855039	11	5271671	11	HBG2	rs12042181	1	213088494	HBG1	HBG2	6.78	0.08	0.52	0.21	
HBG1	ILMN_1796678	11	rs2855039	11	5271671	11	HBG2	rs12042181	1	213088494	HBG1	HBG2	6.78	0.08	0.52	0.21	
HBG1	ILMN_1796678	11	rs2855039														

Continued on next page



Table S1 – continued from previous page

[illegible]

Continued on next page

Table S1 – continued from previous page

[illegible]

Continued on next page

Table S1 – continued from previous page

Gene ID <sup>a</sup>	Expression trait		SNP 1		SNP 2		Interaction statistic / -log <sub>10</sub> p-values			
	Probe ID <sup>b</sup>	Chr.	rs ID	Chr.	Pos/Mb <sup>c</sup>	Association <sup>d</sup>	rs ID	Chr.	Pos/Mb <sup>c</sup>	Association <sup>d</sup>
REBE	ILMN-1802380	1	rs4982958	14	24987865		rs301819	1	8501786	REBE
REBE	ILMN-1802380	1	rs7697290	4	135248366		rs301819	1	8501786	REBE
REBE	ILMN-2327795	1	rs11085829	19	13174312		rs301819	1	8501786	REBE
REBE	ILMN-2327795	1	rs3852011	3	112844086	RNASE6	rs301819	1	8501786	REBE
RNASE6	ILMN-1780533	14	rs11628398	14	8106521		rs11628398	14	100601327	RNASE6
RNASE6	ILMN-1780533	14	rs6003134	19	8106521		rs11628398	14	100601327	RNASE6
RNASE6	ILMN-1794726	17	rs2382330	17	4875566		rs11706900	3	36348908	
RNF167	ILMN-1794726	17	rs400658	17	4839930	RNF167	rs11706900	3	36348908	
RNFEP	ILMN-1738347	1	rs1107121	21	46127349		rs2819365	1	201983242	
RNFEP	ILMN-1738347	1	rs8071611	17	67153586		rs2819365	1	201983242	
RPL13	ILMN-2413278	16	rs352935	16	89048580		rs2965817	16	89513234	
RPL23AP7	ILMN-2222730	12	rs1401202	14	50320056		rs4848261	2	114450028	RPL23AP7
RPL36AL	ILMN-2186933	14	rs3007033	14	50320056	RPL36AL	rs17450530	9	138035083	
RPL36AL	ILMN-2186933	14	rs4009028	14	50020817	RPL36AL	rs1502991	6	66137260	
RPL8	ILMN-1764721	8	rs2958482	8	143984615	RPL8	rs1619856	1	234585790	
RPL8	ILMN-1764721	8	rs4143674	20	4741304		rs2958482	8	143984615	
SEC13	ILMN-3297880	3	rs4889214	16	80913946		rs696221	3	10342876	SEC13
SEC13	ILMN-3297880	3	rs17085428	3	83388015		rs7695	1	136147326	SEC13
SES3	ILMN-1702787	11	rs12147460	14	104412137		rs684856	11	94906111	SES3
SES3	ILMN-1694027	11	rs355391	15	46391793	SES3	rs684856	11	94906111	SES3
SES3	ILMN-1694027	11	rs684856	15	46391793		rs7004947	8	134606425	PPBP
SH3BGL2	ILMN-1694027	11	rs10838191	11	43893658		rs1354034	3	56849749	PPBP
SH3BGL2	ILMN-1767664	6	rs2345385	5	4683899		rs1354034	3	56849749	PPBP
SH3BGL2	ILMN-1767664	6	rs6645364	4	88280592		rs1745517	9	131785369	SH3BGL2
SH3BGL2	ILMN-2158336	9	rs1034290	21	18196922	SIRPG	rs6842739	14	6042830	
SIRPG	ILMN-2158336	9	rs1355883	20	1512549		rs367035	17	15233826	SLC22A18
SIRPG	ILMN-2158336	9	rs1355883	20	1512549		rs367035	17	15233826	SLC22A18
SLC22A18	ILMN-2382605	11	rs11673260	19	5215198	SLC22A18	rs367035	17	15233826	SLC22A18
SLC22A18	ILMN-2382605	11	rs367035	19	5215198	SLC22A18	rs367035	17	15233826	SLC22A18
SLC22A18	ILMN-2382605	11	rs367035	19	5215198	SLC22A18	rs367035	17	15233826	SLC22A18
SLC41A3	ILMN-236111	3	rs1912136	11	29236743		rs771703	3	12587558	SLC41A3
SLC41A3	ILMN-236111	3	rs698508	8	14233774	SLC41A3	rs771703	3	12587558	SLC41A3
SLC45A4	ILMN-1658639	13	rs198005	17	5502091		rs7701916	5	174598073	SLC45A4
SLC46A3	ILMN-1775553	1	rs803259	15	97030923		rs10911353	1	18249303	SLC46A3
SMO7	ILMN-1775553	1	rs803259	15	97030923		rs10911353	1	18249303	SMO7
SMO7	ILMN-1775553	1	rs803259	15	97030923		rs10911353	1	18249303	SMO7
SNHG8	ILMN-1775553	20	rs11677215	20	4161500	SMOX	rs11677215	20	4161500	SNHG8
SNHG8	ILMN-1775553	20	rs11677215	20	4161500	SMOX	rs11677215	20	4161500	SNHG8
SNHG8	ILMN-1775553	20	rs11677215	20	4161500	SMOX	rs11677215	20	4161500	SNHG8
SNORD14A	ILMN-1790381	4	rs150620	15	93050233		rs214097	4	19225940	SNORD14A
SNORD14A	ILMN-1790381	4	rs150620	15	93050233		rs214097	4	19225940	SNORD14A
SNORD14A	ILMN-1790381	4	rs150620	15	93050233		rs214097	4	19225940	SNORD14A
SNORD89	ILMN-3238663	2	rs2634462	11	17329127		rs6186334	11	1701557	SNORD89
SNORD89	ILMN-3238663	2	rs2634462	11	17329127		rs6186334	11	1701557	SNORD89
SNORD89	ILMN-3238663	2	rs2634462	11	17329127		rs6186334	11	1701557	SNORD89
SNORD89	ILMN-3238663	2	rs2634462	11	17329127		rs6186334	11	1701557	SNORD89
SNUPN	ILMN-1733932	15	rs2135064	5	26778066	SNUPN	rs6186334	11	1701557	SNUPN
SNUPN	ILMN-1733932	15	rs2135064	5	26778066	SNUPN	rs6186334	11	1701557	SNUPN
SNUPN	ILMN-2364535	15	rs1346466	21	46376528		rs17185362	16	81888905	SNUPN
SPATA5L1	ILMN-1729179	15	rs1346466	21	46376528		rs17185362	16	81888905	SPATA5L1
SPATA5L1	ILMN-1729179	15	rs1346466	21	46376528		rs17185362	16	81888905	SPATA5L1
STARD10	ILMN-2170752	11	rs2221406	19	41117869		rs1477550	15	45652086	STARD10
STARD10	ILMN-2170752	11	rs2221406	19	41117869		rs1477550	15	45652086	STARD10
STARD10	ILMN-2170752	11	rs2221406	19	41117869		rs1477550	15	45652086	STARD10
STARD10	ILMN-2170752	11	rs2221406	19	41117869		rs1477550	15	45652086	STARD10
STYXL1	ILMN-2345142	20	rs4073164	14	104947517	SULF2	rs1006620	11	72509713	STYXL1
STYXL1	ILMN-2345142	20	rs4073164	14	104947517	SULF2	rs1006620	11	72509713	STYXL1
STYXL1	ILMN-2345142	20	rs4073164	14	104947517	SULF2	rs1006620	11	72509713	STYXL1
SULT1A4	ILMN-2336133	16	rs1463965	18	74332954		rs392994	4	180439236	SULT1A4
SULT1A4	ILMN-2336133	16	rs1463965	18	74332954		rs392994	4	180439236	SULT1A4
SULT1A4	ILMN-2336133	16	rs1463965	18	74332954		rs392994	4	180439236	SULT1A4
SURF6	ILMN-1778032	9	rs6099626	20	40119768		rs3785354	16	28550667	SURF6
SURF6	ILMN-1778032	9	rs6099626	20	40119768		rs3785354	16	28550667	SURF6
SYTL2	ILMN-2336609	11	rs1375719	13	10341078		rs3118663	9	136281753	SYTL2
SYTL2	ILMN-2336609	11	rs1375719	13	10341078		rs3118663	9	136281753	SYTL2
THBS3	ILMN-1804663	1	rs1939875	11	95422867		rs485485	11	85495269	THBS3
THBS3	ILMN-1804663	1	rs1939875	11	95422867		rs485485	11	85495269	THBS3
THBS3	ILMN-1804663	1	rs1939875	11	95422867		rs485485	11	85495269	THBS3
TIPRL	ILMN-1781457	1	rs2823245	21	16745523		rs2049805	1	155194980	TIPRL
TIPRL	ILMN-1781457	1	rs2823245	21	16745523		rs2049805	1	155194980	TIPRL
TIPRL	ILMN-1781457	1	rs2823245	21	16745523		rs2049805	1	155194980	TIPRL
TIPRL	ILMN-1781457	1	rs2823245	21	16745523		rs2049805	1	155194980	TIPRL

Continued on next page

Table S1 – continued from previous page

Gene ID <sup>a</sup>		Expression trait		SNP 1		SNP 2		Interaction statistic / -log <sub>10</sub> p-values		Distance / Mb <sup>h</sup>					
TMED4	Probe ID <sup>b</sup>	Chr.	rs ID	Chr.	Pos / Mb <sup>c</sup>	Association <sup>d</sup>	rs ID	Chr.	Pos / Mb <sup>c</sup>		Association <sup>d</sup>	BSGS <sup>e</sup>	Fehrmann <sup>f</sup>	EGCUT <sup>g</sup>	Meta <sup>g</sup>
TMED4	ILMN-1804148	7	rs19340400	11	132389627		rs17725246	7	44581986	TMED4	3.70	0.06	1.34	0.70	
TMEM149	ILMN-1786426	19	rs28390113	21	47248981		rs8106959	19	36219525	TMEM149	8.11	0.16	0.48	0.26	
TMEM149	ILMN-1786426	19	rs5762235	22	27925288		rs8106959	19	36219525	TMEM149	6.79				
TMEM149	ILMN-1786426	19	rs6090518	20	43207005		rs8106959	19	36219525	TMEM149	11.09	0.76			
TMEM149	ILMN-1786426	19	rs807491	19	36268923	SNX26	rs7254601	19	36147315	TMEM149	12.16	81.55	45.78	145.78	0.122
TMEM149	ILMN-1786426	19	rs8106959	19	36219525	TMEM149	rs10254601	9	133025756		8.02	1.55	3.09	3.07	
TMEM149	ILMN-1786426	19	rs8106959	19	36219525	TMEM149	rs10937361	3	188395746		8.30	0.40	0.99	0.80	
TMEM149	ILMN-1786426	19	rs8106959	19	36219525	TMEM149	rs1401098	12	128884559		7.37	2.41	1.00	2.52	
TMEM149	ILMN-1786426	19	rs8106959	19	36219525	TMEM149	rs1557335	18	64268976		6.95	0.08	0.07	0.03	
TMEM149	ILMN-1786426	19	rs8106959	19	36219525	TMEM149	rs17719594	14	90932398		6.93	3.06	0.77	2.87	
TMEM149	ILMN-1786426	19	rs8106959	19	36219525	TMEM149	rs1843357	8	13822381		6.21	3.72	3.33	6.00	
TMEM149	ILMN-1786426	19	rs8106959	19	36219525	TMEM149	rs2351458	4	113317583		7.30	0.04	9.61	8.00	
TMEM149	ILMN-1786426	19	rs8106959	19	36219525	TMEM149	rs2539000	7	147619772		6.70	1.57	1.52	2.27	
TMEM149	ILMN-1786426	19	rs8106959	19	36219525	TMEM149	rs2731711	5	171792273		5.92	0.19	0.33	0.19	
TMEM149	ILMN-1786426	19	rs8106959	19	36219525	TMEM149	rs471128	11	129595460		8.89	0.90	3.62	3.51	
TMEM149	ILMN-1786426	19	rs8106959	19	36219525	TMEM149	rs6718480	2	233879066		8.55	3.31	5.15	7.36	
TMEM149	ILMN-1786426	19	rs8106959	19	36219525	TMEM149	rs6926382	2	161683974		5.80	3.06	8.80	10.72	
TMEM149	ILMN-1786426	19	rs8106959	19	36219525	TMEM149	rs7213338	17	80357420		5.49	0.07	3.14	2.10	
TMEM149	ILMN-1786426	19	rs8106959	19	36219525	TMEM149	rs914940	1	242889492		6.22	3.36	6.96	9.20	
TMEM149	ILMN-1786426	19	rs8106959	19	36219525	TMEM149	rs9509428	13	21473952		9.44	0.10	5.75	4.47	
TMEM63A	ILMN-1719649	1	rs1254086	13	72890603		rs4149226	1	226027323	TMEM63A	5.60	0.64	0.12	0.32	
TMEM80	ILMN-1788482	11	rs1548475	6	58058246		rs4963126	11	65845	TMEM80	5.79	0.11	0.15	0.07	
TMPO3	ILMN-1683811	7	rs1537146	9	4859303		rs10488630	7	128593948	IRF5	5.61	1.03	0.17	0.62	
TRNA2A	ILMN-1731043	7	rs1997693	20	22287303		rs11770192	7	23498358	IRF5	8.23	3.19	1.89	4.09	
TRAPPC4	ILMN-1814650	11	rs1278523	13	113531675		rs3916581	11	11888787	TRAPPC4	5.52	0.28	0.40	0.29	
TRAPPC5	ILMN-2372639	19	rs17159840	19	7758194	TRAPPC5	rs10059004	5	166970604	TRAPPC4	5.52	0.93	0.01	0.36	
TRAPPC5	ILMN-2372639	19	rs17159840	19	7758194	TRAPPC5	rs1023095	8	132022957	TRAPPC4	5.97	0.21	1.60	1.07	12.131
TRAPPC5	ILMN-2372639	19	rs17159840	19	7758194	TRAPPC5	rs1375714	6	156404902	TRAPPC5	6.92	0.37	0.87	0.68	
TRAPPC5	ILMN-2372639	19	rs17159840	19	7758194	TRAPPC5	rs1393299	1	24329791	TRAPPC5	7.79	0.12	0.18	0.09	
TRAPPC5	ILMN-2372639	19	rs17159840	19	7758194	TRAPPC5	rs17763599	19	2369415	TRAPPC5	6.43	0.63	0.47	0.58	
TRAPPC5	ILMN-2372639	19	rs17159840	19	7758194	TRAPPC5	rs4968328	17	57495457	TRAPPC5	6.51	0.21	0.24	0.16	
TRAPPC5	ILMN-2372639	19	rs17159840	19	7758194	TRAPPC5	rs7313362	12	129644342	TRAPPC5	6.38	0.50	0.34	0.44	
TRAPPC5	ILMN-2372639	19	rs17159840	19	7758194	TRAPPC5	rs7694997	4	9947811	TRAPPC5	7.08	0.04	0.65	0.25	
TRAPPC5	ILMN-2372639	19	rs17159840	19	7758194	TRAPPC5	rs7800935	7	146690926	TRAPPC5	5.86	0.20	0.36	0.22	
TRAPPC5	ILMN-2372639	19	rs17159840	19	7758194	TRAPPC5	rs856638	14	85439550	TRAPPC5	6.27	0.15	0.33	0.16	
TRAPPC5	ILMN-2372639	19	rs30708	22	22740855		rs17159840	19	7758194	TRAPPC5	7.58	0.85	0.78	1.01	
TRAPPC5	ILMN-2372639	19	rs3916995	19	45128451		rs17159840	19	7758194	TRAPPC5	7.73	0.51	0.55	0.56	
TRAPPC5	ILMN-2372639	19	rs6040514	20	11272861		rs10179572	2	228504503	TRAPPC5	8.10	0.14	0.02	0.02	
TRAPPC5	ILMN-2372639	19	rs7246264	19	7762978		rs12921440	16	30408795	TRAPPC5	6.71	0.14	0.26	0.13	
TRAPPC5	ILMN-2372639	19	rs7246264	19	7762978		rs1887778	3	134635088	TRAPPC5	7.34	0.08	0.86	0.40	
TRAPPC5	ILMN-2372639	19	rs7246264	19	7762978		rs963354	3	157393770	TRAPPC5	7.05	0.08	0.90	0.69	
TREM1	ILMN-1688231	6	rs10862975	12	85749398		rs2395771	6	41264577	TREM1	5.42	0.36	0.90	0.69	
TREM1	ILMN-1688231	6	rs2527180	17	158808416		rs2395771	6	41264577	TREM1	5.92	0.11	0.25	0.11	
TRIM38	ILMN-1697971	6	rs2527180	17	158808416		rs2032447	6	26044369	TRIM38	6.46	0.04	0.91	0.39	
TSPAN14	ILMN-1785060	10	rs968726	7	27194634	MYBPC3	rs10748526	10	82273079	TSPAN14	6.00	0.04	0.91	0.39	
TSPAN32	ILMN-1718621	11	rs10838738	11	47663049	MYBPC3	rs12800098	11	2317951	TSPAN32	5.01	0.07	0.18	0.06	
TSPAN32	ILMN-2389070	11	rs12800098	11	2317951	TSPAN32	rs620607	6	137947208	TSPAN32	5.51	0.07	0.18	0.06	
TMPO	ILMN-323126	22	rs140522	22	50971266	ECGF1	rs1198819	2	238746880	TMPO	6.34	0.07	0.18	0.06	45.345
TMPO	ILMN-323126	22	rs470119	22	50966914	ECGF1	rs4783126	16	85147633	TMPO	6.13	0.07	0.18	0.06	

Continued on next page

Table S1 – continued from previous page

Expression trait			SNP 1			SNP 2			Interaction statistic <sup>f</sup> / -log <sub>10</sub> p-values			Distance / Mb <sup>h</sup>		
Gene ID <sup>a</sup>	Probe ID <sup>b</sup>	Chr.	rs ID	Chr.	Pos / Mb <sup>c</sup>	Association <sup>d</sup>	rs ID	Chr.	SNP-2	Association <sup>d</sup>	BSGS <sup>e</sup>	Fehrmann <sup>f</sup>	EGCUT <sup>g</sup>	Meta <sup>g</sup>
UBASH3A	LMN-2338348	21	rs1893592	21	43855067	UBASH3A	rs7201194	16	83600397		5.91	0.59	0.42	0.52
UBASH3A	LMN-2338348	21	rs1893592	21	43855067	UBASH3A	rs7201194	16	83600397		6.01	0.48	1.29	1.10
USP36	LMN-1697227	17	rs2279308	17	76794981	USP36	rs7225546	17	75151717		5.71	0.03	0.14	0.03
VASP	LMN-1743646	19	rs1264226	19	40063167		rs2276470	19	45974668		5.09	0.94	5.14	4.95
VNN2	LMN-1678939	6	rs10435352	7	103252718		rs1883613	6	133077063	VNN2	5.64	0.84	0.15	0.46
VNN2	LMN-1678939	6	rs10435352	7	103252718		rs1883613	6	133077063	VNN2	5.44	0.39	0.69	0.57
VNN2	LMN-1678939	6	rs134447	22	49927332		rs1883617	6	133072650	VNN2	5.72			
VNN2	LMN-1678939	6	rs134447	22	49927332		rs1883617	6	133072650	VNN2	5.77	0.33	0.19	0.19
VNN3	LMN-1678939	6	rs216495	11	16834510		rs1883617	6	133072650	VNN2	5.77	0.33	0.19	0.19
VNN3	LMN-1678939	6	rs10278073	7	151662184		rs2267952	6	133067782	VNN3	6.44	0.16	0.74	0.41
VNN3	LMN-1804935	6	rs1443946	8	73006453		rs2267952	6	133067782	VNN3	5.74	0.23	0.48	0.31
VNN3	LMN-1804935	6	rs1443946	8	73006453		rs2267952	6	133067782	VNN3	6.44	0.31	0.17	0.17
VNN3	LMN-1804935	6	rs348462	9	75547169		rs2267952	6	133067782	VNN3	5.82	0.03	0.19	0.04
VNN3	LMN-1804935	6	rs7157055	14	83262064		rs2267952	6	133067782	VNN3	6.12	0.73	1.15	1.21
VNN3	LMN-2387680	6	rs2823165	21	5694253		rs2267952	6	133067782	VNN3	6.12	0.73	1.15	1.21
VNN3	LMN-2387680	6	rs2823165	21	5694253		rs2267952	6	133067782	VNN3	4.83	0.46	0.05	0.16
VNN3	LMN-2387680	6	rs9596457	13	51692548		rs2267952	6	133067782	VNN3	4.83	0.46	0.05	0.16
VSTM1	LMN-1763455	19	rs9596457	13	51692548	VSTM1	rs4532100	18	71024750		5.60	0.53	0.54	0.57
VSTM1	LMN-1763455	19	rs10500316	19	54553697	VSTM1	rs4532100	18	71024750		5.71	0.48	1.17	0.26
VSTM1	LMN-1763455	19	rs10500316	19	54553697	VSTM1	rs7895870	10	123095249		5.71	0.48	1.17	0.26
VSTM1	LMN-1763455	19	rs9628570	22	30261219	VSTM1	rs7895870	10	123095249		5.71	0.48	1.17	0.26
VSTM1	LMN-1763455	19	rs9628570	22	30261219	VSTM1	rs7895870	10	123095249		5.71	0.48	1.17	0.26
WDR48	LMN-1762103	3	rs1388935	3	188927822		rs10500316	19	54553697	VSTM1	5.88	0.81	1.38	1.47
WDR48	LMN-1762103	3	rs1388935	3	188927822		rs10500316	19	54553697	VSTM1	5.88	0.81	1.38	1.47
WDR48	LMN-1762103	3	rs1887778	9	134635088		rs6778963	3	39091812	WDR48	5.88	0.19	0.13	0.09
WDR48	LMN-1762103	3	rs1887778	9	134635088		rs6778963	3	39091812	WDR48	5.88	0.19	0.13	0.09
WDR6	LMN-1669484	3	rs9554833	13	102624790	RAPGEF1	rs883349	3	39067925	WDR48	6.34	0.57	1.35	1.22
WDR6	LMN-1669484	3	rs9554833	13	102624790	RAPGEF1	rs883349	3	39067925	WDR48	6.34	0.57	1.35	1.22
XAF1	LMN-2330573	17	rs12362253	11	123371708		rs7619193	3	39044116	WDR6	5.85	0.18	0.61	0.35
XAF1	LMN-2330573	17	rs12362253	11	123371708		rs7619193	3	39044116	WDR6	5.85	0.18	0.61	0.35
XAF1	LMN-2330573	17	rs1535031	21	9673170	XAF1	rs11715581	3	49194331		4.86	1.64	1.43	2.25
ZFP90	LMN-1684628	16	rs9064476	17	37040648		rs12591171	15	68179799		5.48	2.38	0.17	1.63
ZFP90	LMN-1684628	16	rs9064476	17	37040648		rs12591171	15	68179799		5.48	2.38	0.17	1.63
ZNF500	LMN-1700238	16	rs4282723	22	48283177		rs182968	16	93573945	ZFP90	5.79	0.09	0.36	0.10
ZNF500	LMN-1700238	16	rs4282723	22	48283177		rs182968	16	93573945	ZFP90	5.79	0.09	0.36	0.10
ZYX	LMN-1701875	7	rs6056281	20	89353122		rs2290560	16	4799041	ZNF500	5.29	0.67	0.27	0.46
ZYX	LMN-1701875	7	rs6056281	20	89353122		rs2290560	16	4799041	ZNF500	5.29	0.67	0.27	0.46
ZYX	LMN-1701875	7	rs6056281	20	89353122		rs2242601	7	143093824	ZYX	6.04	0.26	0.01	0.05

<sup>a</sup> Phenotypes are expression levels of RefSeq Genes<sup>b</sup> Illumina probe ID used to measure gene expression<sup>c</sup> Physical SNP position in base pairs (HG19)<sup>d</sup> RefSeq Gene ID of gene expression level that is influenced by the SNP (BSGS discovery dataset, significance threshold = 1.29 × 10<sup>-11</sup>)<sup>e</sup> Interaction - log<sub>10</sub> p-value from discovery dataset<sup>f</sup> Interaction - log<sub>10</sub> p-value from replication dataset<sup>g</sup> Interaction - log<sub>10</sub> p-value from meta analysis of replication datasets only<sup>h</sup> Distance in Mb between interacting SNPs for *cis-cis* acting SNP pairs<sup>i</sup> p-values are absent if the interaction did not pass the QC filtering in the replication dataset<sup>j</sup> Meta analysis p-values are absent if the interaction did not pass the QC filtering in either replication dataset



Table S2: **Estimation of additive and non-additive variance components from pedigree information** Taken from previous analysis in Powell et al 2013<sup>22</sup>

Gene	Probe	Additive		Non-additive	
		Variance	s.e.	Variance	s.e.
NAPRT1	ILMN_1710752	0.37	0.03	0.14	0.05
TMEM149	ILMN_1786426	0.41	0.04	0.09	0.04
MBNL1	ILMN_2313158	0.18	0.03	0.11	0.04
TRAPPC5	ILMN_2372639	0.32	0.04	0.13	0.05
CAST	ILMN_1717234	0.31	0.03	0.10	0.04

Table S3: **Concordance of sign of epistatic variance components between discovery and replication datasets**

Test	Interactions <sup>a</sup>	Dataset	$n^b$	Expected <sup>c</sup>	Observed <sup>d</sup>	$p$ -value
1 <sup>e</sup>	All	EGCUT	434	217.00	306	$6.69 \times 10^{-18}$
		Fehrmann	434	217.00	278	$5.04 \times 10^{-9}$
		Both	434	108.50	221	$5.56 \times 10^{-31}$
	Significant	EGCUT	30	15.00	25	$3.25 \times 10^{-4}$
		Fehrmann	30	15.00	24	$1.43 \times 10^{-3}$
		Both	30	7.50	22	$3.76 \times 10^{-8}$
2 <sup>f</sup>	All	EGCUT	434	54.25	92	$4.22 \times 10^{-7}$
		Fehrmann	434	54.25	79	$6.18 \times 10^{-4}$
		Both	434	6.78	30	$2.55 \times 10^{-11}$
	Significant	EGCUT	30	3.75	19	$9.46 \times 10^{-11}$
		Fehrmann	30	3.75	19	$9.46 \times 10^{-11}$
		Both	30	0.47	18	$2.23 \times 10^{-25}$
3 <sup>g</sup>	All	EGCUT	1133	566.50	775	$7.10 \times 10^{-36}$
		Fehrmann	1133	566.50	726	$1.90 \times 10^{-21}$
		Both	1133	283.25	562	$1.39 \times 10^{-70}$
	Significant	EGCUT	73	36.50	55	$1.69 \times 10^{-5}$
		Fehrmann	73	36.50	55	$1.69 \times 10^{-5}$
		Both	73	18.25	46	$7.86 \times 10^{-12}$

<sup>a</sup> “All” denotes 434 discovery interactions and “Significant” denotes 30 interactions with significant replication  $p$ -values

<sup>b</sup> Number of tests for concordance

<sup>c</sup> Expected number of concordant cases under the null hypothesis of no interactions

<sup>d</sup> Observed number of concordant cases

<sup>e</sup> The sign of the most significant epistatic variance component in discovery is the same as the corresponding variance component in the replication data.

<sup>f</sup> The largest epistatic variance component in the discovery is the same as in the replication with the same sign in both.

<sup>g</sup> The sign of all epistatic variance components in the discovery with  $p < 0.05$  are the same as the corresponding variance components in the replication data.

Table S4: **Concordance of sign of epistatic variance components between discovery and replication datasets using test 4**

Interactions <sup>a</sup>	Dataset	$n^b$	0 <sup>c</sup>	1 <sup>c</sup>	2 <sup>c</sup>	3 <sup>c</sup>	4 <sup>c</sup>	$p$
Expected <sup>d</sup>	-	-	0.06	0.25	0.38	0.25	0.06	-
All	EGCUT	434	0.06	0.22	0.41	0.23	0.08	0.194
All	Fehrman	434	0.07	0.22	0.39	0.24	0.08	0.385
All	Combined	868	0.07	0.22	0.40	0.23	0.08	0.0448
Significant	EGCUT	30	0.07	0.03	0.30	0.33	0.27	$4.72 \times 10^{-4}$
Significant	Fehrman	30	0.03	0.07	0.33	0.27	0.30	$6.69 \times 10^{-4}$
Significant	Combined	60	0.05	0.05	0.32	0.30	0.28	$5.49 \times 10^{-8}$

<sup>a</sup> “All” denotes 434 discovery interactions and “Significant” denotes 30 interactions with significant replication  $p$ -values.

<sup>b</sup> Number of tests for concordance.

<sup>c</sup> Proportion of tests that have 0, 1, 2, 3 or 4 concordant signs between discovery and replication.

<sup>d</sup> Expected proportion of concordant signs under the null hypothesis of no epistasis.

Table S5: Details on linkage disequilibrium and relative positions of all discovery interactions with SNPs on the same chromosome

Chr	Gene	SNP 1	SNP 2	Position 1	Position 2	Distance / Mb	$R^2$	$D'$
19	TMEM149	rs807491	rs7254601	36268923	36147315	0.122	0.000	0.001
17	FN3KRP	rs898095	rs9892064	80890638	80827903	0.063	0.063	0.088
21	CSTB	rs9979356	rs3761385	45230974	45198355	0.033	0.041	0.066
3	MBNL1	rs16864367	rs13079208	152234166	152116652	0.118	0.041	0.117
10	ADK	rs2395095	rs10824092	76446305	75929517	0.517	0.013	0.020
11	CTSC	rs7930237	rs556895	88117962	88077479	0.040	0.012	0.045
17	GAA	rs11150847	rs12602462	78153130	78146016	0.007	0.000	0.001
8	NAPRT1	rs2123758	rs3889129	144663661	144613680	0.050	0.053	0.060
1	LAX1	rs1891432	rs10900520	203877662	203780591	0.097	0.065	0.106
18	MBP	rs8092433	rs4890876	74747424	74732087	0.015	0.035	0.053
11	SNORD14A	rs2634462	rs6486334	17339127	17015557	0.324	0.008	0.012
21	C21ORF57	rs9978658	rs11701361	48027084	47764477	0.263	0.032	0.065
16	RPL13	rs352935	rs2965817	89648580	89513234	0.135	0.054	0.060
19	ATP13A1	rs4284750	rs873870	19810050	19738554	0.071	0.008	0.015
2	NCL	rs7563453	rs4973397	232301670	232291471	0.010	0.027	0.029
5	HNRPH1	rs6894268	rs4700810	179032488	178991794	0.041	0.000	0.001
19	VASP	rs1264226	rs2276470	46063167	45974668	0.088	0.018	0.022
7	TRA2A	rs7776572	rs11770192	23528927	23498358	0.031	0.064	0.064
21	PRMT2	rs2839372	rs11701058	48063862	47776382	0.287	0.100	0.122
12	OAS1	rs13311	rs2072133	113448652	113409260	0.039	0.002	0.016
16	N4BP1	rs12444224	rs11649236	87580855	48632478	38.948	0.007	0.021
5	CAST	rs12719343	rs7733671	125369113	96000269	29.369	0.001	0.001
7	DNAJB6	rs2286842	rs3779589	157216093	157163614	0.052	0.005	0.006
1	OVGP1	rs10802822	rs1264898	240132968	111992823	128.140	0.008	0.030
20	CD93	rs2868504	rs1884655	37771578	23074375	14.697	0.000	0.002
11	PHCA	rs493642	rs10736812	123097386	76708086	46.389	0.002	0.008
21	MX1	rs459498	rs8130120	42795027	29363604	13.431	0.000	0.000
16	AKTIP	rs2896940	rs13332406	57721127	53489705	4.231	0.000	0.001
17	CDK5R1	rs9905940	rs11655031	46614102	30833162	15.781	0.000	0.000
2	CYBRD1	rs888427	rs7591849	172368120	160112881	12.255	0.000	0.000
8	HMBOX1	rs587639	rs7837237	132725731	28876221	103.850	0.001	0.001
11	TRAPPC4	rs1793823	rs3916581	131018917	118887887	12.131	0.001	0.002
12	PEX5	rs10444467	rs4329748	128052636	7364442	120.688	0.000	0.000
12	FLJ20489	rs17615703	rs3782908	117036766	48169526	68.867	0.001	0.002
16	PRKCB1	rs2188355	rs10492793	23867776	12639800	11.228	0.000	0.000
14	MRPL52	rs1950857	rs3811188	26710271	23299135	3.411	0.002	0.004
17	C17ORF60	rs9907897	rs7405659	63502633	59874129	3.629	0.004	0.011
6	FLJ43093	rs6906101	rs13214069	36667610	32705248	3.962	0.000	0.000
19	TRAPPC5	rs17159840	rs17763599	7758194	2369415	5.389	0.000	0.000
22	PISD	rs715572	rs6518754	33234931	32097775	1.137	0.001	0.003
12	DIP2B	rs871257	rs12427378	117994348	51074199	66.920	0.001	0.001
12	GPR162	rs2272500	rs2707210	79685913	6902002	72.784	0.003	0.005
17	USP36	rs2279308	rs7225546	76794981	75151717	1.643	0.000	0.000